Eddy Viscosity Models in Variational Multiscale Methods for Turbulent Flow Simulations

Mingyang Liu

Master Thesis

Supervisor: Univ.-Prof. Dr. Volker John
Second Reviewer: Dr. Alfonso Caiazzo

Fachbereich Mathematik und Informatik
Freie Universität Berlin

Berlin, December 19, 2019

Contents

1 Introduction

The objective of this thesis is to discuss the eddy viscosity model for the turbulent flows. The start of the study is the derivation of the Navier-Stokes equations. We use the principle of the Newton's second law, i.e., the conservation of mass and the conservation of momentum, to form the Navier-Stokes equations. In the same time, we transformed the equations into dimensionless Navier-Stokes equations to convenience our study in the mathematical sense. We defined the domain that we worked on to be a three dimensional hexahedron with periodic boundary conditions.

We defined the type of flows that we are interested in, which is the turbulent incompressible flows. Because of the unknown term ‚Reynolds stress tensor' of the Navier-Stokes equations, we seek for a computable term to replace it. Another point is the difficulty of the numerical study. We noticed that not all the scales can be simulated by the finite element method we applied. Because the eddies are not always large enough to be represented on the grid, i.e., the discretization of the small eddies is impossible to achieve. Hence, we introduced two solutions in this thesis, the Smagorinsky model and the Verstappen model. In the thesis, we derived both of the Smagorinsky model and the Verstappen model. And we explained in details, for the Verstappen model, the existence of the eddy viscosity constant, and the reason we applied it into our models.

In the end, we performed several experiments with the code ParMooN. We proved that the Verstappen model has a better behavior, in the sense of two quantities of interest, whcih are the difference to the mean and the root mean squared tensor. We also noticed that the Smagorinsky model with van Driest damping is for the quantity of interest ‚Reynolds stress tensor' a better simulation. The conclusion comes from the comparison among all three best choices of the models, the Smagorinsky model, the Smagorinsky model with van Driest damping and the Verstappen model.

2 Navier-Stokes Equations

Navier-Stokes equations are models that tell us how the flow within a domain behaves as time flies. The equations come from the Newton's second law and the conservation of mass.

In general, according to Newton's second law, we know that the force is equal to mass times acceleration. Suppose we have a domain Ω that flow lives in, and we choose an arbitrary ω from Ω. We say that the fluid in ω has a defined mass, this mass is defined by its density $\rho[\mathrm{kg/m^3}]$. Besides, we represent the route of the fluid as a 3D route function, by the definition, the velocity and acceleration could be calculated as the first and second derivatives of the route function. Regardless of the route function, we could have a vector of velocity $\boldsymbol{v}(t,\boldsymbol{x}) = (v_x(t,\boldsymbol{x}), v_y(t,\boldsymbol{x}), v_z(t,\boldsymbol{x}))[\mathrm{m/s}]$. We note that the velocity depends on t and $\boldsymbol{x}$. And for each direction of the coordinate, we have a velocity scale. Therefore, we can define acceleration by doing derivation on the velocity: $a(t,\boldsymbol{x}) = d\boldsymbol{v}(t,\boldsymbol{x})/dt[\mathrm{m/s^2}]$.

2.1 Conservation of mass

In this section, we want to study the mass of the flow in an arbitrary domain ω. Since we know nothing about the material of the flow, then we suppose that the density may change as time and coordinate do. Hence we define the density $\rho = \rho(t,\boldsymbol{x})[kg/m^3]$. Moreover, the mass of the flow in ω is

$$m(t) = \int_\omega \rho(t,\boldsymbol{x}) d\boldsymbol{x}.$$

According to the conservation of mass, the total mass in a domain doesn't change in time. The derivative of mass $m(t)$ should be equal to 0, because $m(t)$ is constant. Hence,

$$\begin{aligned}\frac{d}{d\mathrm{t}} m(t) &= \frac{d}{dt}\int_\omega \rho(t,\boldsymbol{x}) d\boldsymbol{x} \\ &= \int_\omega \frac{d}{dt}\rho(t,\boldsymbol{x}) d\boldsymbol{x} \\ &= 0.\end{aligned}$$

Since the rate of change of mass in ω must be equal to the flux of mass $\rho\boldsymbol{v}(t,\boldsymbol{x})$ across

the boundary $\partial\omega$ of ω. Therefore,

$$\begin{aligned}\frac{d}{d\mathrm{t}}m(t) &= \int_\omega \frac{d}{d\mathrm{t}}\rho(t,\boldsymbol{x})d\boldsymbol{x} + \int_{\partial\omega}(\rho\boldsymbol{v})(t,\boldsymbol{s})\cdot\boldsymbol{n}ds \\ &= \int_\omega \frac{\partial}{\partial\mathrm{t}}\rho(t,\boldsymbol{x}) + \nabla\cdot(\rho\boldsymbol{v})(t,\boldsymbol{x})d\boldsymbol{x}.\end{aligned} \tag{2.1}$$

Because of the conservation of mass, i.e., equation (2.1), and the arbitrary choice of ω we have the first equation of Navier-Stokes equations

$$\partial_\mathrm{t}\rho(t,\boldsymbol{x}) + \nabla\cdot(\rho\boldsymbol{v})(t,\boldsymbol{x}) = 0. \tag{2.2}$$

Furthermore, if the choice of ω depends on time, we can get an equation similar to (2.1), by using Reynolds Transport theorem [3],

$$\begin{aligned}\frac{d}{dt}\int_{\omega(t)}\rho(t,\boldsymbol{x})d\boldsymbol{x} &= \int_{\omega(t)}\partial_\mathrm{t}\rho(t,\boldsymbol{x})d\boldsymbol{x} + \int_{\partial\omega(t)}(\rho\boldsymbol{v}\cdot\boldsymbol{n})(t,s)ds \\ &\overset{\text{div thm}}{=} \int_{\omega(t)}\partial_\mathrm{t}\rho(t,\boldsymbol{x})d\boldsymbol{x} + \int_{\omega(t)}\nabla\cdot(\rho\boldsymbol{v})(t,\boldsymbol{x})d\boldsymbol{x} \\ &= \int_{\omega(t)}(\partial_\mathrm{t}\rho(t,\boldsymbol{x}) + \nabla\cdot(\rho\boldsymbol{v})(t,\boldsymbol{x}))d\boldsymbol{x}.\end{aligned}$$

Now we consider a special case, namely the case of an incompressible and homogeneous fluid. We define such flows (for instance of water or air) are incompressible and homogeneous, if the density of such flows do not change as time or position changes. To describe it mathematically, from (2.1), we have

$$\frac{d}{d\mathrm{t}}\rho(t,\boldsymbol{x}) = \partial_\mathrm{t}\rho(t,\boldsymbol{x}) + \nabla\cdot(\rho\boldsymbol{v})(t,\boldsymbol{x}) = 0.$$

Since $\rho(t,\boldsymbol{x}) = \rho$ is constant, hence $\partial_\mathrm{t}\rho(t,\boldsymbol{x}) = 0$, and the second term becomes

$$\rho\nabla\cdot\boldsymbol{v}(t,\boldsymbol{x}) = 0.$$

Therefore, one property of incompressible and homogeneous flow is

$$\nabla\cdot\boldsymbol{v}(t,\boldsymbol{x}) = (\partial_x\boldsymbol{v}_1 + \partial_y\boldsymbol{v}_2 + \partial_z\boldsymbol{v}_3)(t,\boldsymbol{x}) = 0.$$

2.2 Conservation of momentum

According to Newton's second law, we can use the conservation of linear momentum to get another equation of Navier-Stokes equations. The linear momentum of the chosen domain Ω is related to density and velocity. If we define the momentum of a unit cubic [m^3] of the flow in unit time [s] to be $\rho\boldsymbol{v}(t,\boldsymbol{x})$ [$\mathrm{kg/s}\cdot\mathrm{m}^2$], then the linear momentum of flow over an arbitrary volume ω is,

$$\boldsymbol{P} = \int_\omega \rho\boldsymbol{v}(t,\boldsymbol{x})d\boldsymbol{x} \quad [\mathrm{kg}\cdot\mathrm{m/s} = \mathrm{N\,s}].$$

Since the linear momentum depends on mass and velocity, we can derive the equation to get Newton's second law.

$$\begin{aligned}\frac{d}{dt}\boldsymbol{P} &= \frac{d}{dt} m \cdot \boldsymbol{v}(t, \boldsymbol{x}) \\ &= m \cdot \frac{d\boldsymbol{v}(t, \boldsymbol{x})}{dt} \\ &= m \cdot \boldsymbol{a}(t, \boldsymbol{x}) \\ &= \boldsymbol{F}.\end{aligned}$$

Let $f_{\text{net}}[\text{N/m}^3]$ be the force density on the domain, then

$$\boldsymbol{F} = m \cdot \boldsymbol{a}(t, \boldsymbol{x}) = \int_\omega \boldsymbol{f}_{\text{net}}(t, \boldsymbol{x}) d\boldsymbol{x}.$$

Therefore we get

$$\frac{d}{dt} \int_\omega \rho \boldsymbol{v}(t, \boldsymbol{x}) d\boldsymbol{x} = \int_\omega \boldsymbol{f}_{\text{net}}(t, \boldsymbol{x}) d\boldsymbol{x}.$$

Similar to equation (2.2), replacing ρ with $\rho\boldsymbol{v}$, we get

$$\begin{aligned}\frac{d}{dt} \int_\omega \rho \boldsymbol{v}(t, \boldsymbol{x}) d\boldsymbol{x} &= \int_\omega \partial_t \rho \boldsymbol{v}(t, \boldsymbol{x}) d\boldsymbol{x} + \int_{\partial\omega} \rho \boldsymbol{v} (\boldsymbol{v} \cdot \boldsymbol{n})(t, s) ds \\ &= \int_\omega \partial_t \rho \boldsymbol{v}(t, \boldsymbol{x}) d\boldsymbol{x} + \int_\omega \nabla \cdot (\rho \boldsymbol{v} \boldsymbol{v}^T)(t, \boldsymbol{x}) d\boldsymbol{x} \\ &= \int_\omega \boldsymbol{f}_{\text{net}}(t, \boldsymbol{x}) d\boldsymbol{x}.\end{aligned}$$

Using the chain rule we get $\nabla \cdot (\rho \boldsymbol{v}\boldsymbol{v}^T) = \rho(\nabla \cdot \boldsymbol{v})\boldsymbol{v}^T + \rho(\boldsymbol{v} \cdot \nabla)\boldsymbol{v}$. Since the flow is incompressible and homogeneous, $\nabla \cdot \boldsymbol{v} = 0$. Replacing this with the term in the integral function, we get

$$\int_\omega \rho(\partial_t \boldsymbol{v} + (\boldsymbol{v} \cdot \nabla)\boldsymbol{v})(t, \boldsymbol{x}) d\boldsymbol{x} = \int_\omega \boldsymbol{f}_{\text{net}}(t, \boldsymbol{x}) d\boldsymbol{x}.$$

Since we choose the domain arbitrarily, we finally get the Navier-Stokes equations as follows,

$$\rho(\partial_t \boldsymbol{v} + (\boldsymbol{v} \cdot \nabla)\boldsymbol{v}) = \boldsymbol{f}_{\text{net}}.$$

We have already arrived pretty close to the final equation. Now we can decompose the force. Since we have not only the force inside the domain ω, but also, we care about the force on the surface of the domain ω. Firstly, we split the force density into two parts, which we call internal force density and external force density. We refer to the external force density as gravity, which is not so difficult to understand as a physical parameter. However, the other internal force density is complicated to measure. We suppose the

force density on the boundary to be a function $\boldsymbol{t}(t,\boldsymbol{x})[N/m^2]$. Then the total measure of the force of the domain ω is

$$\int_\omega \boldsymbol{f}_{\text{net}}(t,\boldsymbol{x})d\boldsymbol{x} \int_\omega \boldsymbol{f}_{\text{ext}}(t,\boldsymbol{x})d\boldsymbol{x} + \int_{\partial\omega} \boldsymbol{t}(t,\boldsymbol{s})d\boldsymbol{s}$$
$$= \int_\omega \boldsymbol{f}_{\text{ext}}(t,\boldsymbol{x})d\boldsymbol{x} + \int_\omega \nabla\cdot\mathbb{S}(t,\boldsymbol{x})d\boldsymbol{x},$$

where $\mathbb{S}(t,\boldsymbol{x})[N/m^2]$ is a 3×3 tensor, which is also named as Cauchy stress tensor, and

$$\boldsymbol{t}(t,\boldsymbol{s}) = \mathbb{S}(t,\boldsymbol{x})\boldsymbol{n}.$$

Therefore, the Navier-Stokes equations can now be written as follows,

$$\rho\partial_t\boldsymbol{v} + \rho(\boldsymbol{v}\cdot\nabla)\boldsymbol{v} - \nabla\cdot\mathbb{S} = \boldsymbol{f}_{\text{ext}}. \tag{2.3}$$

Notice that the Cauchy stress tensor is symmetric, we have six unknown elements in $\mathbb{S}$. We can decompose the Cauchy stress tensor as the sum of viscous stress tensor and pressure diagonal tensor.

$$\mathbb{S} = \mathbb{V} - P\mathbb{I}, \tag{2.4}$$

where $\mathbb{V}$ [N/m^2] is a symmetric tensor, P [Pa] is a pressure vector, $\mathbb{I}$ is identity 3×3 tensor. Since the pressure only acts on the domain in the opposite direction, we use negative sign here.

As for the viscous stress tensor, we define a tensor that depends linearly on the first derivatives of the velocity,

$$\mathbb{V} = a\mathbb{D}(\boldsymbol{v}) + b(\nabla\cdot\boldsymbol{v})\mathbb{I},$$

where

$$\mathbb{D}(\boldsymbol{v}) = \frac{\nabla\boldsymbol{v} + (\nabla\boldsymbol{v})^T}{2}[1/s], \tag{2.5}$$

and $\boldsymbol{v}$ is the vector of velocity. Precisely analog to the Hook's law of solid, one can write the viscous stress tensor in the form,

$$\mathbb{V} = 2\mu\mathbb{D}(\boldsymbol{v}) + (\zeta - \frac{2\mu}{3})(\nabla\cdot\boldsymbol{v})\mathbb{I}, \tag{2.6}$$

where $\mu[kg/m\cdot s]$ is called the first order viscosity and $\zeta[kg/m\cdot s]$ is the second order viscosity. If the fluid is incompressible, then the second term will be vanished. Hence, we have,

$$\mathbb{S} = 2\mu\mathbb{D}(\boldsymbol{v}) - P\mathbb{I}. \tag{2.7}$$

Inserting (2.4) into the Navier-Stokes equations (2.3), we have

$$\begin{aligned}\rho(\partial_t\boldsymbol{v} + (\boldsymbol{v}\cdot\nabla)\boldsymbol{v}) - 2\nabla\cdot\mu\mathbb{D}(v) - \nabla\cdot((\zeta - \frac{2\mu}{3})(\nabla\cdot\boldsymbol{v})\mathbb{I}) + \nabla P = \boldsymbol{f}_{\text{ext}}\,(0,T]\times\Omega \\ \partial_t\rho + \nabla\cdot(\rho\boldsymbol{v}) = 0 \quad (0,T]\times\Omega.\end{aligned} \tag{2.8}$$

If the fluid is incompressible and homogeneous, then insert $\nabla \cdot \boldsymbol{v} = 0$ into (2.8), we have

$$\begin{aligned} \partial_t \boldsymbol{v} + (\boldsymbol{v} \cdot \nabla)\boldsymbol{v} - 2\nu \nabla \cdot \mathbb{D}(\boldsymbol{v}) + \frac{1}{\rho}\nabla P = \frac{\boldsymbol{f}_{\text{ext}}}{\rho} \qquad & (0,T] \times \Omega \\ \nabla \cdot \boldsymbol{v} = 0 \qquad & (0,T] \times \Omega, \end{aligned} \tag{2.9}$$

where $\nu = \frac{\mu}{\rho}[m^2/s]$ is called the kinematic viscosity of the fluid.

The equation in (2.7) gives us the form of Newtonian flows. We define those flows, who obey the following two assumptions as Newtonain flows:

- the Cauchy stress tensor depends only on the first order spatial derivatives of the velocity,
- the Cauchy stress tensor depends linearly on the first order spatial derivatives of the velocity.

It is obvious that the right-hand side of (2.7) fully satisfies the two assumptions above.

2.3 Dimensionless Navier-Stokes equations

For mathematical analysis purposes and numerical simulations, we need to derive the dimensionless Navier-Stokes equations. Firstly, we set several characteristic scales of the flow problem. We define $L[m]$ to be the characteristic length scale, $U[m/s]$ to be the characteristic velocity scale, and $T^*[s]$ to be the characteristic time scale. Suppose the old variables in the Navier-Stokes equations (2.9) are of the form $(t', \boldsymbol{x}')[s, m]$. Then we can reformulate the equations using the following variables:

$$\boldsymbol{x} = \frac{\boldsymbol{x}'}{L}, \qquad \boldsymbol{u} = \frac{\boldsymbol{v}}{U}, \qquad t = \frac{t'}{T^*}.$$

We can rescale the equations by multiplying $\frac{1}{U^2}$ on both sides of the first equation in (2.9), then applying the chain rule to get the rescaled equation. At the same time, after rescale the equation, the time interval and domain are dimensionless. Suppose that the old variables $(t', \boldsymbol{x}')$ live in the domain $(0, T'] \times \Omega'$, then we can now define $T = \frac{T'}{T^*}$ and Ω to be the rescaled domain of Ω'. Hence, we get the rescaled form as follows,

$$\begin{aligned} \frac{L}{UT^*}\partial_t \boldsymbol{u} + (\boldsymbol{u} \cdot \nabla)\boldsymbol{u} - \frac{2\nu}{UL}\nabla \cdot \mathbb{D}(\boldsymbol{u}) + \nabla \frac{P}{\rho U^2} = \frac{L}{\rho U^2}\boldsymbol{f}_{\text{ext}} \qquad & (0,T] \times \Omega \\ \nabla \cdot \boldsymbol{u} = 0 \qquad & (0,T] \times \Omega. \end{aligned} \tag{2.10}$$

The complicated parameters in the equations above will also be replaced by fixed physical parameters, i.e.,

$$p = \frac{P}{\rho U^2}, \qquad \text{Re} = \frac{UL}{\nu}, \qquad \text{St} = \frac{L}{UT^*}, \qquad f = \frac{L}{\rho U^2}\boldsymbol{f}_{\text{ext}},$$

where Re is called Reynolds number, and St is called Strouhal number. Therefore, after inserting the parameters in the Navier-Stokes equations (2.10) we get the incompressible Navier-Stokes equations as follow,

$$\begin{aligned} \mathrm{St}\partial_t \boldsymbol{u} + (\boldsymbol{u}\cdot\nabla)\boldsymbol{u} - \frac{2}{\mathrm{Re}}\nabla\cdot\mathbb{D}(\boldsymbol{u}) + \nabla p = \boldsymbol{f} \qquad & (0,T]\times\Omega \\ \nabla\cdot\boldsymbol{u} = 0 \qquad & (0,T]\times\Omega. \end{aligned} \tag{2.11}$$

We can simplify the notations in (2.11) by using the dimensionless scale $T^* = L/U$ and $\nu = \mathrm{Re}^{-1}$ to get the basic equation for mathematical analysis purpose.

$$\begin{aligned} \partial_t \boldsymbol{u} + (\boldsymbol{u}\cdot\nabla)\boldsymbol{u} - 2\nu\nabla\cdot\mathbb{D}(\boldsymbol{u}) + \nabla p = \boldsymbol{f} \qquad & (0,T]\times\Omega \\ \nabla\cdot\boldsymbol{u} = 0 \qquad & (0,T]\times\Omega. \end{aligned} \tag{2.12}$$

Since $\mathbb{D}(\boldsymbol{u}) = \frac{1}{2}(\nabla\boldsymbol{u} + (\nabla\boldsymbol{u})^T)$, we can replace $\nabla\cdot\mathbb{D}(\boldsymbol{u})$ in (2.12) with simpler form,

$$\begin{aligned} \nabla\cdot\mathbb{D}(\boldsymbol{u}) &= \frac{1}{2}\nabla\cdot(\nabla\boldsymbol{u} + (\nabla\boldsymbol{u})^T) \\ &= \frac{1}{2}(\triangle\boldsymbol{u} + \ nabla(\nabla\cdot\boldsymbol{u})) \\ &= \frac{1}{2}\triangle\boldsymbol{u}. \end{aligned} \tag{2.13}$$

Inserting (2.13) into (2.12) we have,

$$\begin{aligned} \partial_t \boldsymbol{u} + (\boldsymbol{u}\cdot\nabla)\boldsymbol{u} - \nu\triangle\boldsymbol{u} + \nabla p = \boldsymbol{f} \qquad & (0,T]\times\Omega \\ \nabla\cdot\boldsymbol{u} = 0 \qquad & (0,T]\times\Omega. \end{aligned} \tag{2.14}$$

Until now we have already got the general form of Navier-Stokes equations. For example, the velocity and pressure stay unchanged, then the component $\partial_t\boldsymbol{u}$ in (2.14) vanishes, we call such equation as the stationary Navier-Stokes equations.

2.4 Initial and boundary conditions

The Navier-Stokes equations (2.14) contain a first derivative in time and second derivatives in space. We seek for the numerical solutions of the equations. First of all, we will define the initial value $\boldsymbol{u}(0,\boldsymbol{x}) = \boldsymbol{u}_0(\boldsymbol{x})$ at $t = 0$. The initial flow should be divergence free since we have $\nabla\cdot\boldsymbol{u} = 0$.

Generally we have several kinds of boundary conditions, here we only discuss Dirichlet boundary condition. Suppose Ω is bounded and $\Gamma = \partial\Omega$ is the bound of the domain Ω. The Dirichlet boundary condition of the Navier-Stokes equations is defined as

$$\boldsymbol{u}(t,\boldsymbol{x}) = \boldsymbol{g}(t,\boldsymbol{x}), \qquad (0,T]\times\Gamma_{\mathrm{Diri}}, \tag{2.15}$$

where $\Gamma_{\mathrm{Diri}} \subset \Gamma$ is a subset of the boundary in the domain. Specifically, if $\boldsymbol{g}(t,\boldsymbol{x}) = \boldsymbol{0}$, we say that it is a no-slip boundary condition.

Furthermore, another boundary condition, which is called do-nothing boundary condition, is often applied in numerical simulations. As implied before, we define the stress tensor as in (2.7). Hence, the do-nothing boundary condition will be written as

$$\mathbb{S}\boldsymbol{n} = \mathbf{0} \qquad (0,T] \times \Gamma_{\text{Donot}}, \tag{2.16}$$

where $\Gamma_{\text{Donot}} \subset \Gamma$ is a subset of the boundary in the domain.

This boundary condition tells us that the Cauchy stress tensor vanishes on the corresponding boundary. However, the do-nothing boundary condition does not fit for all two-dimensional flow models, such as the Hagen-Poiseuille flow, i.e., the solution of Navier-Stokes equations does not satisfy (2.16). But if we replace the Cauchy stress tensor in (2.7) with the velocity deformation tensor

$$\mathbb{S} = \nu\nabla\boldsymbol{u} - p\mathbb{I}, \tag{2.17}$$

then the do-nothing boundary condition will be satisfied.

On the other hand, if the domain extends to infinitely end, we can apply the periodic boundary condition to the case, which is, we can assume that in the direction of the infinity extension the flow has a period of length l. Therefore, the domain will be defined as $\Omega = (0,l)^d$ and the periodic boundary conditions are given by

$$\boldsymbol{u}(t,\boldsymbol{x} + l\boldsymbol{e}_i) = \boldsymbol{u}(t,\boldsymbol{x}) \qquad \forall (t,\boldsymbol{x}) \in (0,T] \times \Gamma. \tag{2.18}$$

3 Turbulent Flows

3.1 The model of the turbulent flows

The model of dimensionless incompressible Navier-Stokes equations is the basis of numerically simulating turbulent incompressible flows, since the Navier-Stokes equations mainly tell us the fact that the linear momentum and mass are conservative.

Recall the Navier-Stokes equations with initial condition in (2.12), we replace ν with Re^{-1} for simplifying mathematical symbols. The Reynolds number effects the second derivative of the velocity. The range of Reynolds number decides the type of flow. In fact, turbulent flows are characterized by a high Reynolds number. More specifically the Reynolds number of the turbulent flows starts at several thousands. Therefore the viscous term $2\mathrm{Re}^{-1}\nabla \cdot \mathbb{D}(\boldsymbol{u})$ is much smaller than the convective term $\partial_t \boldsymbol{u} + (\boldsymbol{u} \cdot \nabla)\boldsymbol{u}$. Since as the viscosity gets smaller, the system will be more unstable. Hence, a high value of the Reynolds number ensures us the occurrence of turbulent flows.

However, we cannot give an exact definition of what is turbulent. According to physical points of view, we can define those flow structures, which has not only large eddies but also accompany with many very small flow structures, to be turbulent flows. Regardless of the large eddies, we focus on the size of the smallest eddies that occur. The size will be denoted by λ.

The determination of the smallest size of turbulent flows is from the idea of isotropic turbulence, which means that the velocity is statistically stationary under time shifting and statistically homogeneous under coordination rotating or reflecting.

We know that large eddies are unstable and will break up into smaller ones. This process continues until the Reynolds number $\mathrm{Re}(l) = u(l)/\nu$ of the eddies is sufficiently small, such that the eddy is stable and effectively dissipating the kinetic energy. This process is known as energy cascade. We denote the rate of dissipation by $\varepsilon[m^2/s^3]$. In the study of particular flows, we get to know that the value of ε is proportional to U^3/L, and it is independent of the Reynolds number.

We want to describe the size of the smallest eddy. In fact, we cannot yet directly measure the scale. However, from the work of Kolmogorov [5], we can define the so-called Kolmogorov scales via his three hypotheses about turbulent flows:

1. At sufficiently high Reynolds numbers, the small scale turbulent motions are isotropic.

2. In every turbulent flow at sufficiently high Reynolds number, the statistics of the small scale motions have a universal form which is uniquely given by ν and ε.

3. In every turbulent flow at sufficiently high Reynolds number, the statistics of motions of scale l in the range $L \gg l \gg \lambda$ have a universal form uniquely determined by ε and independent of ν.

We define the unique length, velocity and time scales as Kolmogorov scales

$$\lambda = \left(\frac{\nu^3}{\varepsilon}\right)^{\frac{1}{4}}[m], \qquad u_\lambda = (\varepsilon\nu)^{\frac{1}{4}}[m/s], \qquad t_\lambda = \left(\frac{\nu}{\varepsilon}\right)^{\frac{1}{4}}[s]. \tag{3.1}$$

Therefore, the Reynolds number of the eddies of size λ is

$$\mathrm{Re}(\lambda) = \frac{\lambda u_\lambda}{\nu} = 1, \tag{3.2}$$

Since the value of Reynolds number is sufficiently small, the dissipation of the kinetic energy will be effective.

We can also define the rate of dissipation. From (3.3) we can get two equations

$$\begin{aligned} \varepsilon &= \nu \cdot \frac{\varepsilon}{\nu} = \nu\frac{1}{t_\lambda^2}, \\ \varepsilon &= \nu\frac{u_\lambda^2}{\lambda^2}. \end{aligned} \tag{3.3}$$

We can combine both of the right-hand side terms in the equations in (3.3) into one equation, and it gives us the rate of the velocity to the length of Komogorov scale

$$\frac{u_\lambda}{\lambda} = \frac{1}{t_\lambda}. \tag{3.4}$$

Because the choice of λ is small, this rate represents an approximation to the spatial derivative of the Kolmogorov scales' velocity, which is the velocity gradient. From (2.17) we observe that the velocity gradient is bounded uniformly with respect to the Reynolds number. Then we can estimate the size of the Kolmogorov scales. Since

$$\frac{\lambda}{L} = \left(\frac{\nu^3}{\varepsilon}\right)^{\frac{1}{4}} \cdot \frac{1}{L} \sim \left(\frac{\nu^3 L}{U^3}\right)^{\frac{1}{4}} \cdot \frac{1}{L} = \left(\frac{\nu^3}{L^3U^3}\right)^{\frac{1}{4}} = \mathrm{Re}^{-\frac{3}{4}},$$

where L is the length scale, we can neglect the term to have

$$\lambda \sim \mathrm{Re}^{-\frac{3}{4}}. \tag{3.5}$$

Numerical simulations are based on discretizations, which use meshes to compute an approximation of solutions to the Navier-Stokes equations. However, the value of the Kolmogorov scale raises the problem of the mesh size, i.e., the eddies of the smallest size cannot be simulated with the meshes, they are far more micro as the meshes are. Therefore we cannot get a direct numerical simulation with the help of a standard FEM method.

Furthermore, we may as well notice that flows at high Reynolds number have different behaviors in dimension two and three. We define $\boldsymbol{\omega} = \nabla \times \boldsymbol{u}$ to be the vorticity. We can apply the vorticity term in the Navier-Stokes equation and suppose the external force is zero. Then we have

$$\partial_t \boldsymbol{\omega} - \mathrm{Re}^{-1} \nabla \cdot \mathbb{D}(\boldsymbol{\omega}) + (\boldsymbol{u} \cdot \nabla)\boldsymbol{\omega} - (\boldsymbol{\omega} \cdot \nabla)\boldsymbol{u} = 0. \tag{3.6}$$

Since the Reynolds number is high, the second term will be ignored. Hence we get the conservation form of vorticity to be

$$\frac{D\boldsymbol{\omega}}{Dt} = \partial_t \boldsymbol{\omega} + (\boldsymbol{u} \cdot \nabla)\boldsymbol{\omega} \simeq (\boldsymbol{\omega} \cdot \nabla)\boldsymbol{u}. \tag{3.7}$$

From the equation we can see that the change of $\boldsymbol{\omega}$ depends on $\nabla \boldsymbol{u}$. It implies that in turbulent three-dimensional flows, the vortex stretching exists and it is an important feature of the flows. But in dimension two, we cannot have the equation above. Since the vorticity does not equal to zero in the third term and the velocity gradient is not zero in the first two terms as well. We cannot observe any vortex stretching. Thus the two-dimensional flow is not the same as turbulent flows in three dimensions. It is also a reason that we always want the simulation to be established in the three-dimensional space.

3.2 The classical large eddy simulation

The classical large eddy simulation (LES) provides us with a model of filtering out the small eddies in the turbulent flows and modeling their effect on the large scales and computing the behavior of the large eddy scales, such that we can apply this methodology in the Navier-Stokes equations to get numerical solutions.

Since the elements we refer to are vector-valued functions and tensor-valued functions, we should at first give the notations of inner product of two vector-valued functions and Frobenius norm of matrices. We say that the inner product of two functions $\boldsymbol{u}$ and $\boldsymbol{v}$ in the Lebesgue space $L^2(\Omega)$ is

$$(\boldsymbol{u}, \boldsymbol{v}) = \int_\Omega \boldsymbol{u}(\boldsymbol{x})\boldsymbol{v}(\boldsymbol{x}) d\boldsymbol{x}.$$

And the Frobenius norm of a matrix $A \subset \mathbb{R}^{n \times n}$ is

$$\|A\|_F = (A : A)^{\frac{1}{2}} = \left(\sum_{i,j=1}^{n} a_{ij}^2 \right)^{\frac{1}{2}}.$$

The basic approach of LES is to define scales by filtering. The large scales are defined by doing convolution of the velocity with a filter function $g(\cdot)$. The filter function $g(\cdot)$ can help us with filtering out small eddy scales. Therefore, if we have a domain $\Omega = \mathbb{R}^d$ $(d > 1)$ of the turbulent flow, we can define the large scale velocity field in the form of

$$\bar{\boldsymbol{u}}(\boldsymbol{y}) = \frac{1}{\delta(\boldsymbol{y})^d} \int_{\mathbb{R}^d} g\left(\frac{\boldsymbol{y} - \boldsymbol{x}}{\delta(\boldsymbol{y})} \right) \boldsymbol{u}(\boldsymbol{x}) d\boldsymbol{x}, \tag{3.8}$$

and the large scale pressure has the form

$$\bar{p}(\boldsymbol{y}) = \frac{1}{\delta(\boldsymbol{y})^d} \int_{\mathbb{R}^d} g\left(\frac{\boldsymbol{y}-\boldsymbol{x}}{\delta(\boldsymbol{y})}\right) p(\boldsymbol{x}) d\boldsymbol{x}, \tag{3.9}$$

where the function $\delta(\boldsymbol{y})$ gives us all eddies that are of size at least $\delta(\boldsymbol{y})$. With the help of (3.8) and (3.9), we can define the small scales to be

$$(\boldsymbol{u'}, p') = (\boldsymbol{u} - \bar{\boldsymbol{u}}, p - \bar{p}). \tag{3.10}$$

We can simulate the large eddies by inserting $(\bar{\boldsymbol{u}}, \bar{p})$ into the Navier-Stokes equations. Since convolution is a linear operator, we can get the equation by averaging the general Navier-Stokes equations. Hence, we have

$$\begin{aligned} \overline{\partial_t \boldsymbol{u}} - 2\mathrm{Re}^{-1}\overline{\nabla \cdot \mathbb{D}(\boldsymbol{u})} + \overline{\nabla \cdot (\boldsymbol{u}\boldsymbol{u}^T)} + \overline{\nabla p} = \bar{f} \qquad & (0,T] \times \mathbb{R}^d \\ \overline{\nabla \cdot \boldsymbol{u}} = 0 \qquad & (0,T] \times \mathbb{R}^d \\ \bar{\boldsymbol{u}}(0,\cdot) = \overline{\boldsymbol{u}_0} \qquad & \mathbb{R}^d. \end{aligned} \tag{3.11}$$

Furthermore, if we interchange the averaging operators with differentiation operators, we can get the results with the Reynolds stress tensor, which is called space averaged Navier-Stokes equations, as below

$$\begin{aligned} \partial_t \bar{\boldsymbol{u}} - 2\mathrm{Re}^{-1}\nabla \cdot \mathbb{D}(\bar{\boldsymbol{u}}) + \nabla \cdot (\bar{\boldsymbol{u}}\bar{\boldsymbol{u}}^T) + \nabla \cdot \mathcal{R}(\boldsymbol{u},\boldsymbol{u}) + \nabla \bar{p} = \bar{f} \qquad & (0,T] \times \mathbb{R}^d \\ \nabla \cdot \bar{\boldsymbol{u}} = 0 \qquad & (0,T] \times \mathbb{R}^d \\ \bar{\boldsymbol{u}}(0,\cdot) = \overline{\boldsymbol{u}_0} \qquad & \mathbb{R}^d, \end{aligned} \tag{3.12}$$

where

$$\mathcal{R}(\boldsymbol{u},\boldsymbol{u}) = \overline{\boldsymbol{u}\boldsymbol{u}^T} - \bar{\boldsymbol{u}}\bar{\boldsymbol{u}}^T. \tag{3.13}$$

The Reynolds stress tensor composes of two averaging tensors. The space-averaged Navier-Stokes equations are not closed. Because the divergence of the Reynolds stress tensor is not defined in terms of $\bar{\boldsymbol{u}}$. We will decompose it into two parts and observe the properties. One choice is to construct the Reynolds stress tensor in the following form

$$\mathcal{R}(\boldsymbol{u},\boldsymbol{u}) - \frac{\mathrm{tr}(\mathcal{R}(\boldsymbol{u},\boldsymbol{u}))}{3} \cdot \mathbb{I} = -2\nu_T \mathbb{D}(\bar{\boldsymbol{u}}), \tag{3.14}$$

where ν_T is called the turbulent viscosity, and the right-hand side is called eddy viscosity model. We name this form of equation (3.14) as the Boussinesq hypothesis [6].

The purpose of the construction is to add the diagonal term to the pressure $\bar{p}$, which is

$$\bar{p} := \bar{p} + \frac{\mathrm{tr}(\mathcal{R}(\boldsymbol{u},\boldsymbol{u}))}{3} \cdot \mathbb{I}. \tag{3.15}$$

3.2.1 The Smagorinsky model

In the last section, we notice that the right-hand side of (3.14) gives us an unknown new term, the turbulent viscosity ν_T. Usually, the turbulent viscosity depends on the solution, hence the new term is nonlinear. We need to model the turbulent viscosity. On the other side, we know that $\varepsilon \sim U^3/L$, where ε is the dissipation rate. We assume now that for every length scale L_* we have a relationship between this term and the velocity scales U_*. Hence, we have

$$\varepsilon \sim \frac{U_{\text{int}}^3}{L_{\text{int}}}, \qquad \varepsilon \sim \frac{U_\delta^3}{\delta}, \tag{3.16}$$

where we define L_{int} to be the integral length scale and U_{int} to be the corresponding velocity scale. We can also use δ to denote the filter width. Hence, we get the relationship between U_{int} and U_δ is

$$U_\delta \sim \left(\frac{\delta}{L_{\text{int}}}\right)^{\frac{1}{3}} U_{\text{int}}. \tag{3.17}$$

Since for smallest eddies, we define the Reynolds number equals to 1. Then we have

$$\text{Re}(\delta) = \frac{\delta U_\delta}{\nu_T} = 1. \tag{3.18}$$

Hence we have the viscosity term, together with (3.17), in the form of

$$\nu_{\text{T}} = \delta U_\delta \sim U_{\text{int}} L_{\text{int}}^{-\frac{1}{3}} \delta^{\frac{4}{3}}. \tag{3.19}$$

We also assume that the integral velocity scale depends linearly on the deformation tensor of the filtered velocity, i.e.,

$$U_{\text{int}} \sim L_{\text{int}} \|\mathbb{D}(\bar{\boldsymbol{u}})\|_F. \tag{3.20}$$

Now we insert this term into (3.19), with an approximation of $L_{\text{int}} \sim \delta$, and an constant coefficient, to get

$$\nu_{\text{T}} = C_S \delta^2 \|\mathbb{D}(\bar{\boldsymbol{u}})\|_F \tag{3.21}$$

where

$$\text{tr}(\mathbb{D}^2(\cdot)) = \|\mathbb{D}(\cdot)\|_F = 2q(\cdot). \tag{3.22}$$

From now on we get a model of the turbulent viscocity ν_T with respect to δ. In this subsection, we state the Smagorinsky model, which gives us a solution to model the dissipation rate of the Reynolds stress tensor. The diagonal components of the viscocity stress tensor is added to the pressure $\bar{p}$. We only need to consider the dissipation rate of the right-hand side term of (3.14) i.e., $\nabla \cdot (-\nu_T \mathbb{D}(\bar{\boldsymbol{u}}))$. If we insert (3.21) into the dissipation term, we get

$$-\nabla \cdot (C_S \delta^2 \|\mathbb{D}(\bar{\boldsymbol{u}})\|_F) \mathbb{D}(\bar{\boldsymbol{u}})), \tag{3.23}$$

where C_S is the dimensionless Smagorinsky coefficient, and δ refers to the local mesh width.

We can denote the space-averaged velocity and pressure $(\bar{\boldsymbol{u}}, \bar{p})$ with their approximations $(\mathbf{w}, r)$ to get the momentum balance of the Smagorinsky model in the domain $(0, T] \times \Omega$ as follows

$$\partial_t \mathbf{w} - 2\nabla \cdot ((\nu + C_S \delta^2 \|\mathbb{D}(\mathbf{w})\|_F)\mathbb{D}(\mathbf{w})) + (\mathbf{w} \cdot \nabla)\mathbf{w} + \nabla r = \boldsymbol{f}. \tag{3.24}$$

In the paper of [4], we mentioned that the Smagorinsky LES model can cause too much energy dissipation near the walls. We define a non-dimensional wall coefficient $y^+ = y\boldsymbol{u}^*/\boldsymbol{v}$, where $\boldsymbol{u}^* = \tau/\rho$ is the friction velocity at the nearest wall. Hence, y^+ defines different layers from the wall. In this case, we introduce a damping factor in the viscous sub-layer, which is inside viscous wall region $y^+ < 5$, and the Reynolds shear stress is negligible. According to the law of the wall, we can derive the viscosity model of the Smagorinsky LES model with van Driest damping as follows,

$$\nu_T = C_S \delta^2 \|\mathbb{D}(\bar{\boldsymbol{u}})\|_F \left(1 - \exp\left(\frac{-y^+}{A}\right)\right)^2,$$

where $A = 26$, and C_S is the same as in equation (42).

These models predict the dynamics of filtered turbulent flows. However, we can only apply it to the case of turbulent flows, since the perturbance term does not vanish if turbulent no longer exists. In the next section, we will introduce the Verstappen model which fixes this defect.

3.2.2 The Verstappen model

The Verstappen model is an alternative model to the Smagorinsky eddy viscosity model. According to the Kolmogorov hypotheses, the smallest eddies have a universal form, and they are uniquely given by the viscosity ν. The idea of the Verstappen model is to build a sub-filter, filtering out the sub-filter scales in order to control the kinetic energy of the fluctuation by its upper bound, which is the L^2 norm of the velocity gradient. This process is called damping. In this model, we will discuss the evolution of sub-filter eddies. We know that it is difficult to describe the dynamic of the eddies, which have even smaller size than the sub-filter scale. Hence, the Verstappen model gives us an assumption to describe the dynamic of the sub-filter eddies instead of looking into the real development.

In this section, we will continue with the space averaged Navier-Stokes equation (3.12). We use $\bar{\boldsymbol{u}}$ to represents the space averaged functions, where the filter involved the operation of integration. The function $\bar{\boldsymbol{u}}\bar{\boldsymbol{u}}^T - \overline{\boldsymbol{u}\boldsymbol{u}^T}$ depends on both $\bar{\boldsymbol{u}}$ and $\boldsymbol{u}$, and it has the property of non-linearity and convection. Instead, we approximate the residual term by applying a closure model $\tau(\boldsymbol{v})$, where

$$\tau(\boldsymbol{v}) = -2\nu_e \mathbb{D}(\boldsymbol{v}). \tag{3.25}$$

We denote $\boldsymbol{v}$ to be the velocity field of the eddy viscosity model equation, and get the following form,

$$\partial_t \boldsymbol{v} + (\boldsymbol{v} \cdot \nabla)\boldsymbol{v} + \nabla \tilde{p} - 2\nu \nabla \cdot \mathbb{D}(\boldsymbol{v}) = -\nabla \cdot \tau(\boldsymbol{v}). \tag{3.26}$$

The replacement of $\bar{\boldsymbol{u}}$ with $\boldsymbol{v}$ is to stress the difference between the variables in two different models.

Here, we must emphasize that $\tau(\boldsymbol{v}) \neq -\mathcal{R}(\boldsymbol{u},\boldsymbol{u}) = \bar{\boldsymbol{u}}\bar{\boldsymbol{u}}^T - \overline{\boldsymbol{u}\boldsymbol{u}^T}$. Because we cannot give a close form of $\tau(\boldsymbol{v})$. Therefore, in the Smagorinsky model, we define the closure model as in (41). In the Verstappen model, we no longer use this formula but define a new filtering operator,

$$\bar{\boldsymbol{v}} = \frac{1}{|\Omega_\delta|}\int_{\Omega_\delta} \boldsymbol{v}(x,t)dx, \tag{3.27}$$

which is known as a box filter. This box filter calculates the average of the velocity in the domain Ω_δ. To be precise, we consider an arbitrary domain Ω_δ with its diameter δ. Furthermore, we assume that the solution $\boldsymbol{v}$ has periodic boundary conditions on Ω_δ. We are aware of the fact that the solution field $\boldsymbol{v}$ is not generally periodic on the boundary of the domain Ω_δ. In our calculations, the periodic boundary conditions are necessary and δ is the smallest scale that we can observe. In the meantime, this assumption can help us with eliminating the boundary terms while doing integration.

We seek for a close form of the kinetic energy and its upper-bound. Therefore, we introduce a test function $\boldsymbol{v}' = \boldsymbol{v} - \bar{\boldsymbol{v}}$ that represents small eddies, which means, the size of the eddies in this residual field are smaller than the diameter of the domain. The test function helps us to find out the close form of the kinetic energy. By doing weak formulation of (3.26) with the test function in the domain Ω_δ, we obtain,

$$(\partial_t \boldsymbol{v}, \boldsymbol{v}') + \big((\boldsymbol{v}\cdot\nabla)\,\boldsymbol{v}, \boldsymbol{v}'\big) + (\nabla\tilde{p}, \boldsymbol{v}') - (2\nu\nabla\cdot\mathbb{D}(\boldsymbol{v}), \boldsymbol{v}') = (2\nabla\cdot(\nu_e\mathbb{D}(\boldsymbol{v})), \boldsymbol{v}'). \tag{3.28}$$

Since the equation (3.28) contains both $\boldsymbol{v}$ and $\boldsymbol{v}'$, we want to get rid of multi-variables. Hence, we can derive easily from the test function to get $\boldsymbol{v} = \boldsymbol{v}' + \bar{\boldsymbol{v}}$. And we already know that the solution field $\boldsymbol{v}$ is in the vector field of incompressible and homogeneous flows. Therefore, we have the divergence of the velocity is zero, i.e., $\nabla\cdot\boldsymbol{v} = \nabla\cdot(\boldsymbol{v}' + \bar{\boldsymbol{v}}) = 0$. According to the definition of the box filter, $\bar{\boldsymbol{v}}$ is a constant for any arbitrary chosen domain, then we get the divergence of the constant vector $\bar{\boldsymbol{v}}$ is zero, i.e., $\nabla\cdot\bar{\boldsymbol{v}} = 0$. Because the divergence operator is linear, we can finally reach the divergence of the residual field is zero, i.e., $\nabla\cdot\boldsymbol{v}' = 0$. Therefore, from (3.28) we have the following calculation of the weak formulation. Since

$$\frac{d}{dt}(\boldsymbol{v}', \boldsymbol{v}') = (\partial_t\boldsymbol{v}', \boldsymbol{v}') + (\boldsymbol{v}', \partial_t\boldsymbol{v}') = 2(\partial_t\boldsymbol{v}', \boldsymbol{v}'), \tag{3.29}$$

the first term on the left-hand side can be decomposed into

$$\begin{aligned}(\partial_t\boldsymbol{v}, \boldsymbol{v}') &= (\partial_t\bar{\boldsymbol{v}}, \boldsymbol{v}') + (\partial_t\boldsymbol{v}', \boldsymbol{v}')\\ &= (\partial_t\bar{\boldsymbol{v}}, \boldsymbol{v}') + \frac{1}{2}\frac{d}{dt}(\boldsymbol{v}', \boldsymbol{v}')\\ &= (\partial_t\bar{\boldsymbol{v}}, \boldsymbol{v}') + \frac{d}{dt}\int_{\Omega_\delta}\frac{1}{2}\|\boldsymbol{v}'\|^2 dx.\end{aligned} \tag{3.30}$$

We notice that the integral part of the equation (3.30) is the kinetic energy of the residual field $\boldsymbol{v}'$.

Because of our assumption of periodic boundary conditions, we will eliminate the pressure component by doing integration by parts as below,

$$\begin{aligned}(\nabla\tilde{p}, \boldsymbol{v}') &= \int_{\partial\Omega_\delta} \tilde{p}\cdot\boldsymbol{v}'\cdot\boldsymbol{n}\,ds - (\nabla\cdot\boldsymbol{v}', \tilde{p}) \\ &= -(\nabla\cdot\boldsymbol{v}', \tilde{p}) \\ &= 0.\end{aligned} \tag{3.31}$$

We can apply equation (2.13) to reduce the weak form of the component $2\nabla\cdot\mathbb{D}(\boldsymbol{v})$ to $\nabla\cdot\nabla\boldsymbol{v}$. And also we can integrate by parts to get

$$\begin{aligned}-(2\nu\nabla\cdot\mathbb{D}(\boldsymbol{v}), \boldsymbol{v}') &= -\nu(\nabla\cdot\nabla\boldsymbol{v}, \boldsymbol{v}') \\ &= -\int_{\partial\Omega_\delta} \nabla\boldsymbol{v}\cdot\boldsymbol{v}'\cdot\boldsymbol{n}\,ds + \nu(\nabla\boldsymbol{v}, \nabla\boldsymbol{v}') \\ &= \nu(\nabla\boldsymbol{v}, \nabla\boldsymbol{v}') \\ &= \nu(\nabla\bar{\boldsymbol{v}}, \nabla\boldsymbol{v}') + \nu(\nabla\boldsymbol{v}', \nabla\boldsymbol{v}') \\ &= \nu(\nabla\bar{\boldsymbol{v}}, \nabla\boldsymbol{v}') + \nu\int_{\Omega_\delta} \|\nabla\boldsymbol{v}'\|^2 dx.\end{aligned} \tag{3.32}$$

The same calculation is performed to the weak form of the component of $\nu_e\mathbb{D}(\boldsymbol{v})$. Under the assumption that ν_e is constant, we have the following equation,

$$\begin{aligned}(\nabla\cdot\nu_e\mathbb{D}(\boldsymbol{v}), \boldsymbol{v}') &= \nu_e(\nabla\cdot\mathbb{D}(\boldsymbol{v}), \boldsymbol{v}') \\ &= -\frac{\nu_e}{2}(\nabla\boldsymbol{v}, \nabla\boldsymbol{v}') \\ &= -\frac{\nu_e}{2}(\nabla\bar{\boldsymbol{v}}, \nabla\boldsymbol{v}') - \frac{\nu_e}{2}\int_{\Omega_\delta} \|\nabla\boldsymbol{v}'\|^2 dx.\end{aligned} \tag{3.33}$$

In the paper [9], the components of equation (3.28) will be replaced by equations (3.30) to (3.33). And a term is introduced as an integration of the energy, which refers to as the complete energy transfers from $\bar{\boldsymbol{v}}$ to the residual field $\boldsymbol{v}'$, i.e., $\int_{\Omega_\delta} T(\bar{\boldsymbol{v}}, \boldsymbol{v}')dx$. And it will be used to substitute all the terms that contain both $\bar{\boldsymbol{v}}$ and $\boldsymbol{v}'$ after inserting the equations (3.30) to (3.33)into the equation (3.28). Therefore, we will get an equation for the dynamics of the sub-grid scales as follows,

$$\frac{d}{dt}\int_{\Omega_\delta} \|\boldsymbol{v}'\|^2 dx = -\nu\int_{\Omega_\delta} \frac{1}{2}\|\nabla\boldsymbol{v}'\|^2 dx + \int_{\Omega_\delta} T(\bar{\boldsymbol{v}}, \boldsymbol{v}')dx - \nu_e\int_{\Omega_\delta} \frac{1}{2}\|\nabla\boldsymbol{v}'\|^2 dx. \tag{3.34}$$

From the equation (3.34), we observe that the kinetic energy is related to the L^2 norm of the velocity gradient. In order to damp the velocity gradient, we assume that the eddy viscosity can be chosen to balance the energy transfer from $\bar{\boldsymbol{v}}$ to $\boldsymbol{v}'$, i.e., the last two terms in (3.34) balance. This assumption ensures us that no sub-filter scales in equation (3.26) would be produced. The left equation helps us with finding out the evolution of the kinetic energy of $\boldsymbol{v}'$. Since we have presently

$$\frac{d}{dt}\int_{\Omega_\delta} \frac{1}{2}\|\boldsymbol{v}'\|^2 dx = -\nu\int_{\Omega_\delta} \|\nabla\boldsymbol{v}'\|^2 dx \leq 0. \tag{3.35}$$

On the other hand, according to Poincare's inequality, the dissipation rate of the small scales, which is defined as the integral over L_2 norm of the residual field, has an upper bounded as below,

$$\int_{\Omega_\delta} \|\boldsymbol{v}'\|^2 dx \leq \mathrm{C}_\delta \int_{\Omega_\delta} \|\nabla \boldsymbol{v}'\|^2 dx, \tag{3.36}$$

where C_δ is the Poincare constant and independent of $\boldsymbol{v}$, for every $\boldsymbol{v}$ in the Sobolev space $W^{1,2}(\Omega_\delta)$. It is given by

$$\mathrm{C}_\delta = \left(\frac{\delta}{\pi}\right)^2, \tag{3.37}$$

for a convex domain.

Now we can use (3.36) to bound the twice derivative of the kinetic energy in (3.35) to get

$$\frac{d}{dt}\int_{\Omega_\delta} \|\boldsymbol{v}'\|^2 dx \leq -\frac{2\nu}{\mathrm{C}_\delta}\int_{\Omega_\delta} \|\boldsymbol{v}'\|^2 dx. \tag{3.38}$$

We can regard the left part of equation (56) as a differential inequality, since the right-hand side constantly depends on the differential function itself. We can apply Gronwall's lemma to get

$$\int_{\Omega_\delta} \|\boldsymbol{v}'\|^2(t,x) dx \leq \exp\left(-\frac{2\nu}{\mathrm{C}_\delta} t\right) \int_{\Omega_\delta} \|\boldsymbol{v}'\|^2(0,x) dx. \tag{3.39}$$

The inequality states that the kinetic energy of the sub-grid scales decays as fast as $\exp(-2\nu t/\mathrm{C}_\delta)$.

In the case of classical large eddy simulation model, the dissipation rate is denoted by $\int_{\Omega_l}(\nu+\nu_e)\|\nabla \boldsymbol{v}\|^2 dx$, where $l \geq \delta$, and Ω_l is an arbitrary domain with diameter l. Under the consideration of energy transfer, the eddy viscosity should stop the progress from large eddies breaking up and forming small eddies that have scale smaller than δ. Hence the dissipation rate is decreasing at a rate controlled by fluid viscosity ν.

We need to find out the minimum amount of eddy viscosity that satisfies the dissipation condition, which is,

$$\frac{d}{dt}\int_{\Omega_\delta} \frac{1}{2}\|\nabla \boldsymbol{v}\|^2 dx = -\nu \int_{\Omega_\delta} \|\Delta \boldsymbol{v}\|^2 dx \leq 0. \tag{3.40}$$

The determination of the eddy viscosity in this model will be derived in the same way as in equation (3.28), i.e., by taking the L^2 inner product of equation (3.26) with $\Delta \boldsymbol{v}$, and then integration by parts,

$$\frac{d}{dt}\int_{\Omega_\delta} \frac{1}{2}\|\nabla \boldsymbol{v}\|^2 dx = -\nu \int_{\Omega_\delta} \|\Delta \boldsymbol{v}\|^2 dx + \int_{\Omega_\delta} \left((\boldsymbol{v}\cdot\nabla)\boldsymbol{v}\cdot\Delta\boldsymbol{v} - \nu_e\|\Delta\boldsymbol{v}\|^2\right) dx. \tag{3.41}$$

We assume that the velocity $\boldsymbol{v}$ is sufficiently smooth such that all operations performed below are well defined. We choose the solution space of the velocity $\boldsymbol{v}$ to be in the Sobolev space $W^{2,2}(\Omega_\delta)$. Hence, we could derive that $\nabla \boldsymbol{v}$ is in the solution space $W^{1,2}(\Omega_\delta)$. Therefore, the gradient of velocity field satisfies the Poincare inequality as follows,

$$\int_{\Omega_\delta} \|\nabla \boldsymbol{v}\|^2 dx \leq \mathrm{C}'_\delta \int_{\Omega_\delta} \|\Delta \boldsymbol{v}\|^2 dx. \tag{3.42}$$

We can apply Gronwall's lemma once more, together with equation (3.40) to get the upper-bound of the L^2 norm of the velocity gradient,

$$\int_{\Omega_\delta} \|\nabla \boldsymbol{v}\|^2 dx \leq \exp\left(-\frac{2\nu}{\mathrm{C}'_\delta} t\right) \int_{\Omega_\delta} \|\nabla \boldsymbol{v}\|^2(0,x) dx. \tag{3.43}$$

By replacing the right-hand side of (3.36) with the inequality (3.43), we can get the upper bound of the kinetic energy

$$\int_{\Omega_\delta} \|\boldsymbol{v}\|^2 dx \leq \mathrm{C}_\delta \exp\left(-\frac{2\nu}{\mathrm{C}'_\delta} t\right) \int_{\Omega_\delta} \|\nabla \boldsymbol{v}\|^2(0,x) dx. \tag{3.44}$$

Because of equation (3.40), we can cancel out the left-hand side term and the first term on the right-hand side to get

$$\nu_e \int_{\Omega_\delta} \|\Delta \boldsymbol{v}\|^2 dx = \int_{\Omega_\delta} (\boldsymbol{v} \cdot \nabla)\boldsymbol{v} \cdot \Delta \boldsymbol{v} \, dx. \tag{3.45}$$

In the paper [1], the right-hand part of (3.45) is stated to be equal to $4 \int_{\Omega_\delta} r(\boldsymbol{v}) \, dx$, where $r(\boldsymbol{v}) = -\frac{1}{3}\mathrm{tr}(\mathbb{D}^3(\boldsymbol{v})) = -\det \mathbb{D}(\boldsymbol{v})$. Also this symbol is only proved to apply for three-dimensional Navier-Stokes equations. Therefore, we have the following equation

$$\begin{aligned} \int_{\Omega_\delta} (\boldsymbol{v} \cdot \nabla)\boldsymbol{v} \cdot \Delta \boldsymbol{v} \, dx &= 4 \int_{\Omega_\delta} r(\boldsymbol{v}) \, dx \\ &= -4 \int_{\Omega_\delta} \det \mathbb{D}(\boldsymbol{v}) \, dx. \end{aligned} \tag{3.46}$$

In the same time, we define $q(\boldsymbol{\omega}) = \frac{1}{2}\mathrm{tr}(\mathbb{D}^2(\boldsymbol{\omega}))$ with $\boldsymbol{\omega} = \nabla \times \boldsymbol{v}$, as in equation (3.22). Then we can use the identity $\Delta \boldsymbol{v} = -\nabla \times \boldsymbol{\omega} = -\nabla \times \nabla \times \boldsymbol{v}$. And the left-hand side of equation (3.45) would be induced as

$$4 \int_{\Omega_\delta} q(\boldsymbol{\omega}) \, dx = \int_{\Omega_\delta} \|-\nabla \times \boldsymbol{\omega}\|^2 dx = \int_{\Omega_\delta} \|\Delta \boldsymbol{v}\|^2 dx. \tag{3.47}$$

Therefore, together with the definition of box filter in equation (3.27), the value of ν_e can be represented as

$$\nu_e = \frac{\int_{\Omega_\delta} r(\boldsymbol{v}) dx}{\int_{\Omega_\delta} q(\boldsymbol{\omega}) dx} = \frac{\overline{r(\boldsymbol{v})}}{\overline{q(\boldsymbol{\omega})}}. \tag{3.48}$$

The estimation of $\overline{q(\boldsymbol{\omega})}$ is related to the following lemma.

Lemma 1. *Let $\Omega \in R^d$, $d \in \{2, 3\}$, and let $\boldsymbol{v} \in H^1(\Omega)$ with periodic boundary conditions, then it holds*

$$\|\nabla \boldsymbol{v}\|^2_{L^2(\Omega)} = \|\nabla \cdot \boldsymbol{v}\|^2_{L^2(\Omega)} + \|\nabla \times \boldsymbol{v}\|^2_{L^2(\Omega)}. \tag{3.49}$$

Proof. First of all, a direct calculation of vectors, using definitions of the operators ∇, $\nabla\cdot$, $\nabla\times$, tells us (see Lemma 3.155 in [2])

$$\nabla \times (\nabla \times \boldsymbol{v})(x) = -\Delta \boldsymbol{v}(x) + \nabla(\nabla \cdot \boldsymbol{v})(x). \tag{3.50}$$

This equation is transformed to a weak form by multiplication with $\boldsymbol{u} \in H^1(\Omega)$, where $\boldsymbol{u}$ is periodic on the boundary. We get the weak form as follows

$$(\nabla \times (\nabla \times \boldsymbol{v}), \boldsymbol{u}) = -(\Delta \boldsymbol{v}, \boldsymbol{u}) + (\nabla(\nabla \cdot \boldsymbol{v}), \boldsymbol{u}). \tag{3.51}$$

Now we need the transform of the right-hand side of equation (3.51). We can use integration by parts to get

$$(-\Delta \boldsymbol{v}, \boldsymbol{u}) = -\int_{\partial\Omega} \boldsymbol{u} \cdot (\nabla \boldsymbol{v} \cdot \boldsymbol{n})\, ds + (\nabla \boldsymbol{v}, \nabla \boldsymbol{u}), \tag{3.52}$$

$$(\nabla(\nabla \cdot \boldsymbol{v}), \boldsymbol{u}) = \int_{\partial\Omega} (\nabla \cdot \boldsymbol{v}) \boldsymbol{u} \cdot \boldsymbol{n}\, ds - (\nabla \cdot \boldsymbol{v}, \nabla \cdot \boldsymbol{u}). \tag{3.53}$$

Since $\boldsymbol{v}$ is periodic bounded, we can derive that $\nabla \boldsymbol{v}$ and $\nabla \cdot \boldsymbol{v}$ are also periodic. It turns out that the boundary integration vanishes.

This property is explained in details for $d = 2$. We can think about a case in a two-dimensional domain. The bound of this domain is composed of E_1, E_2, E_3 and E_4, which forms a boundary of a two-dimensional rectangle. And the direction of each E_i is referred to as $\boldsymbol{n}_i$, $i = 1, 2, 3, 4$. We have the value of the outflow to be defined as below

$$\begin{aligned}\int_{\partial\Omega} \boldsymbol{u} \cdot (\nabla \boldsymbol{v} \cdot \boldsymbol{n})\, dx &= \int_{E1} + \int_{E2} + \int_{E3} + \int_{E4} \boldsymbol{u} \cdot (\nabla \boldsymbol{v} \cdot \boldsymbol{n})\, dx \\ &= \int_{E1} \boldsymbol{u} \cdot (\nabla \boldsymbol{v} \cdot \boldsymbol{n}_1)\, dx + \int_{E2} \boldsymbol{u} \cdot (\nabla \boldsymbol{v} \cdot \boldsymbol{n}_2)\, dx \\ &\quad + \int_{E3} \boldsymbol{u} \cdot (\nabla \boldsymbol{v} \cdot \boldsymbol{n}_3)\, dx + \int_{E4} \boldsymbol{u} \cdot (\nabla \boldsymbol{v} \cdot \boldsymbol{n}_4)\, dx.\end{aligned} \tag{3.54}$$

Since we have periodic conditions on both $\nabla \boldsymbol{v}$ and $\boldsymbol{u}$, i.e.,$\nabla \boldsymbol{v}|_{E1} = \nabla \boldsymbol{v}|_{E2}$, $\nabla \boldsymbol{v}|_{E3} = \nabla \boldsymbol{v}|_{E4}$ and also $\boldsymbol{u}|_{E1} = \boldsymbol{u}|_{E2}$, $\boldsymbol{u}|_{E3} = \boldsymbol{u}|_{E4}$. In addition, we have $\boldsymbol{n}_1 = -\boldsymbol{n}_2$ and $\boldsymbol{n}_3 = -\boldsymbol{n}_4$.

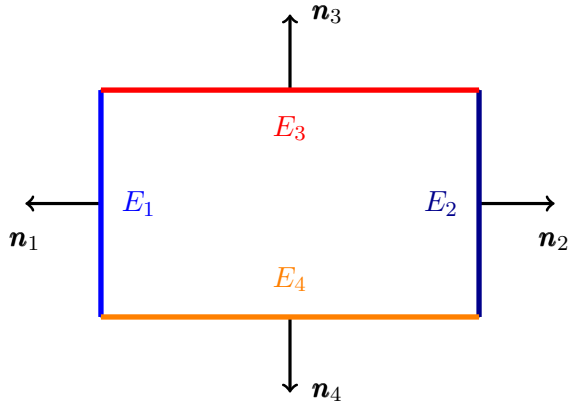

If we insert these terms into equation (3.54), we have the following equation

$$\begin{aligned}\int_{E1}+\int_{E2}+\int_{E3}+\int_{E4}\nabla\boldsymbol{v}\cdot\boldsymbol{u}\cdot\boldsymbol{n}\,dx &= \left(\int_{E1}\nabla\boldsymbol{v}\cdot\boldsymbol{u}\cdot\boldsymbol{n}_1\,dx+\int_{E2}\nabla\boldsymbol{v}\cdot\boldsymbol{u}\cdot\boldsymbol{n}_2\,dx\right)\\ &\quad+\left(\int_{E3}\nabla\boldsymbol{v}\cdot\boldsymbol{u}\cdot\boldsymbol{n}_3\,dx+\int_{E4}\nabla\boldsymbol{v}\cdot\boldsymbol{u}\cdot\boldsymbol{n}_4\,dx\right)\\ &= \left(\int_{E1}\nabla\boldsymbol{v}\cdot\boldsymbol{u}\cdot\boldsymbol{n}_1\,dx-\int_{E2}\nabla\boldsymbol{v}\cdot\boldsymbol{u}\cdot\boldsymbol{n}_1\,dx\right)\\ &\quad+\left(\int_{E3}\nabla\boldsymbol{v}\cdot\boldsymbol{u}\cdot\boldsymbol{n}_3\,dx-\int_{E4}\nabla\boldsymbol{v}\cdot\boldsymbol{u}\cdot\boldsymbol{n}_3\,dx\right)\\ &= 0.\end{aligned} \tag{3.55}$$

Therefore, we only need to prove the following equation

$$(\nabla\times(\nabla\times\boldsymbol{v}),\boldsymbol{u}) = -(\Delta\boldsymbol{v},\boldsymbol{u}), \tag{3.56}$$

where, it is clear to see that,

$$\begin{aligned}\nabla\times(\nabla\times\boldsymbol{v}) &= \nabla\times\begin{pmatrix}(\nabla\times\boldsymbol{v})_1\\(\nabla\times\boldsymbol{v})_2\\(\nabla\times\boldsymbol{v})_3\end{pmatrix}\\ &= \begin{pmatrix}\partial_y(\nabla\times\boldsymbol{v})_3-\partial_z(\nabla\times\boldsymbol{v})_2\\ \partial_z(\nabla\times\boldsymbol{v})_1-\partial_x(\nabla\times\boldsymbol{v})_3\\ \partial_x(\nabla\times\boldsymbol{v})_2-\partial_y(\nabla\times\boldsymbol{v})_1\end{pmatrix}.\end{aligned} \tag{3.57}$$

Hence, under condition that the test function has periodic bound, the weak formulation goes to

$$\begin{aligned}(\nabla\times(\nabla\times\boldsymbol{v}),\boldsymbol{u}) &= -((\nabla\times\boldsymbol{v})_3,\partial_y\boldsymbol{u}_1)+((\nabla\times\boldsymbol{v})_2,\partial_z\boldsymbol{u}_1)-((\nabla\times\boldsymbol{v})_1,\partial_z\boldsymbol{u}_2)\\ &\quad+((\nabla\times\boldsymbol{v})_3,\partial_x\boldsymbol{u}_2)-((\nabla\times\boldsymbol{v})_2,\partial_x\boldsymbol{u}_3)+((\nabla\times\boldsymbol{v})_1,\partial_y\boldsymbol{u}_3)\\ &= ((\nabla\times\boldsymbol{v})_3,\partial_x\boldsymbol{u}_2-\partial_y\boldsymbol{u}_1)+((\nabla\times\boldsymbol{v})_2,\partial_z\boldsymbol{u}_1-\partial_x\boldsymbol{u}_3)\\ &\quad+((\nabla\times\boldsymbol{v})_1,\partial_y\boldsymbol{u}_3-\partial_z\boldsymbol{u}_2)\\ &= (\nabla\times\boldsymbol{v},\nabla\times\boldsymbol{u}).\end{aligned} \tag{3.58}$$

We can now apply integral by parts, and the integrals on opposite boundaries cancel again because of the periodicity of all functions and the derivatives. We can obtain the following equation

$$(\Delta\boldsymbol{v},\boldsymbol{u}) = \int_{\partial\Omega}\nabla\boldsymbol{v}\cdot\boldsymbol{u}\cdot\boldsymbol{n}\,dx-(\nabla\boldsymbol{v},\nabla\boldsymbol{u}) = -(\nabla\boldsymbol{v},\nabla\boldsymbol{u}). \tag{3.59}$$

We can combine equation (3.55), (3.56), (3.58) and (3.59), and insert $\boldsymbol{u}=\boldsymbol{v}$, to obtain

$$(\nabla\times\boldsymbol{v},\nabla\times\boldsymbol{v})+(\nabla\cdot\boldsymbol{v},\nabla\cdot\boldsymbol{v}) = (\nabla\boldsymbol{v},\nabla\boldsymbol{v}), \tag{3.60}$$

which is equivalent to the desired equation (3.49). □

Lemma 2. *If $\boldsymbol{\omega}$ is as $\boldsymbol{v}$ in Lemma 1 with $\boldsymbol{\omega} = \nabla \times \boldsymbol{v}$, then*

$$\|\nabla \boldsymbol{\omega}\|_{L^2(\Omega)} = \|\nabla \times \boldsymbol{\omega}\|_{L^2(\Omega)}. \tag{3.61}$$

Proof. We know that $\boldsymbol{\omega}$ is in the solution field $H^1(\Omega)$ with periodic boundary conditions. We may as well find a $\boldsymbol{v}$ in the same solution field such that $\boldsymbol{\omega} = \nabla \times \boldsymbol{v}$. In the same time, we can prove that equation (3.49) still holds, if we replace $\boldsymbol{v}$ with $\nabla \times \boldsymbol{v}$. Because we define that$\nabla \times \boldsymbol{v} = \begin{pmatrix} \partial_y \boldsymbol{v}_3 - \partial_z \boldsymbol{v}_2 \\ \partial_z \boldsymbol{v}_1 - \partial_x \boldsymbol{v}_3 \\ \partial_x \boldsymbol{v}_2 - \partial_y \boldsymbol{v}_1 \end{pmatrix}$. According to this definition of $\nabla\times$, we have

$$\nabla \cdot (\nabla \times \boldsymbol{v}) = \partial_{yx} \boldsymbol{v}_3 - \partial_{xz} \boldsymbol{v}_2 + \partial_{zy} \boldsymbol{v}_1 - \partial_{xy} \boldsymbol{v}_3 + \partial_{xz} \boldsymbol{v}_2 - \partial_{yz} \boldsymbol{v}_1 = 0. \tag{3.62}$$

Therefore , the term $\|\nabla \cdot (\nabla \times \boldsymbol{v})\|_{L^2(\Omega)} = \|\nabla \cdot \boldsymbol{\omega}\|_{L^2(\Omega)} = 0$, for any $\boldsymbol{\omega}$ in the solution field, combining with the equation (3.49) to get (3.61). □

We can continue the estimation of the equation (3.48). Since the value of eddy viscosity model still depends on both $\boldsymbol{v}$ and $\Delta \boldsymbol{v}$. We can use Poincare inequality to get rid of $\Delta \boldsymbol{v}$ as follows,

$$\begin{aligned} \int_{\Omega_\delta} q(\boldsymbol{\omega})\, dx &= \frac{1}{4} \int_{\Omega_\delta} \|\nabla \times \boldsymbol{\omega}\|^2 dx \\ &= \frac{1}{4} \|\nabla \times \boldsymbol{\omega}\|^2_{L^2(\Omega_\delta)} \\ &\overset{(3.61)}{=} \frac{1}{4} \|\nabla \boldsymbol{\omega}\|^2_{L^2(\Omega_\delta)} \\ &\geq \frac{1}{\mathrm{C}_\delta} \cdot \frac{1}{4} \|\boldsymbol{\omega}\|^2_{L^2(\Omega_\delta)} \\ &= \frac{1}{4\mathrm{C}_\delta} \|\nabla \times \boldsymbol{v}\|^2_{L^2(\Omega_\delta)} \\ &= \frac{1}{4\mathrm{C}_\delta} \int_{\Omega_\delta} \|\nabla \times \boldsymbol{v}\|^2 dx \\ &= \frac{1}{\mathrm{C}_\delta} \int_{\Omega_\delta} q(\boldsymbol{v})\, dx. \end{aligned} \tag{3.63}$$

Inserting equation (3.63) into equation (3.48) gives us an upper-bound of the eddy viscosity model, but only depends on variable $\boldsymbol{v}$

$$\nu_e \leq \mathrm{C}_\delta \frac{\int_{\Omega_\delta} r(\boldsymbol{v}) dx}{\int_{\Omega_\delta} q(\boldsymbol{v}) dx} = \mathrm{C}_\delta \frac{\overline{r(\boldsymbol{v})}}{\overline{q(\boldsymbol{v})}}. \tag{3.64}$$

In the paper [9], the eddy dissipation was derived from a scalar eddy viscosity model. It is also possible to derive it by computing the eddy viscosity ν_e directly from equation (3.64). The problem is that we need to describe the behaviors of r and q in the domain Ω_δ. Because the large-eddy simulation $\boldsymbol{v}$ is represents as $\boldsymbol{v} = \overline{\boldsymbol{v}} + \boldsymbol{v}'$. We can use it to

compute $\overline{r(\boldsymbol{v})}$ and $\overline{q(\boldsymbol{v})}$. We need to notice that $r(\boldsymbol{v})$ can be negative, we would adjust it to $\overline{|r(\boldsymbol{v})|}$ in the case of $r < 0$. We can approximate the LES velocity $\boldsymbol{v}$ by applying approximate deconvolution method, which recovers some of the lost information while filtering. Since $\boldsymbol{v}'$ is the residual of the large eddies, we consider the expansion of $\boldsymbol{v}$ around the average $\overline{\boldsymbol{v}}$, to get $\boldsymbol{v}' \approx -1/24\,\delta^2\Delta\overline{\boldsymbol{v}}$. We can insert the value of $\boldsymbol{v}'$ and apply the definition of inner production to get the following estimation,

$$\begin{aligned}
\overline{q(\boldsymbol{v})} &= \frac{1}{4}\overline{\|\nabla \boldsymbol{v}\|^2} \\
&= \frac{1}{4}\overline{\|\nabla(\overline{\boldsymbol{v}} + \boldsymbol{v}')\|^2} \\
&\approx \frac{1}{4}\overline{\left\|\nabla\left(\overline{\boldsymbol{v}} - \frac{1}{24}\delta^2\Delta\overline{\boldsymbol{v}}\right)\right\|^2} \\
&= \frac{1}{4}\overline{\left(\nabla\overline{\boldsymbol{v}} - \frac{\delta^2}{24}\nabla(\Delta\overline{\boldsymbol{v}}), \nabla\overline{\boldsymbol{v}} - \frac{\delta^2}{24}\nabla(\Delta\overline{\boldsymbol{v}})\right)} \\
&= \frac{1}{4}\left(\overline{(\nabla\overline{\boldsymbol{v}}, \nabla\overline{\boldsymbol{v}})} - \frac{\delta^2}{12}\overline{(\nabla\overline{\boldsymbol{v}}, \nabla(\Delta\overline{\boldsymbol{v}}))} + \left(\frac{\delta^2}{24}\right)^2\overline{(\nabla(\Delta\overline{\boldsymbol{v}}), \nabla(\Delta\overline{\boldsymbol{v}}))}\right).
\end{aligned} \tag{3.65}$$

There are three terms on the right-hand side of the estimation (3.65), we will take the second and third one into consideration. We can apply integration by parts to the second term, to get

$$(\nabla\overline{\boldsymbol{v}}, \nabla(\Delta\overline{\boldsymbol{v}})) = \int_{\partial\Omega} \nabla\overline{\boldsymbol{v}} \cdot \Delta\overline{\boldsymbol{v}} \cdot \boldsymbol{n}\, ds - (\Delta\overline{\boldsymbol{v}}, \Delta\overline{\boldsymbol{v}}). \tag{3.66}$$

Since we have periodic boundary condition on the solution field $\boldsymbol{v}$, and due to the linearity of the integration of the filter, we have also periodic condition on $\nabla\overline{\boldsymbol{v}}$. Hence, the boundary integral in (3.66) equals to 0. Therefore, by applying the Poincare inequality, we have

$$(\nabla\overline{\boldsymbol{v}}, \nabla(\Delta\overline{\boldsymbol{v}})) = -(\Delta\overline{\boldsymbol{v}}, \Delta\overline{\boldsymbol{v}}) \leq -\frac{1}{C_\delta}\|\nabla\overline{\boldsymbol{v}}\|^2. \tag{3.67}$$

Since there is a negative parameter in front of the term in equation (3.65), we would have

$$-\frac{\delta^2}{12}\overline{(\nabla\overline{\boldsymbol{v}}, \nabla(\Delta\overline{\boldsymbol{v}}))} \geq \frac{\delta^2}{12} \cdot \frac{1}{C_\delta}\overline{\|\nabla\overline{\boldsymbol{v}}\|^2}. \tag{3.68}$$

Now, we only need to apply Poincare inequality twice to the third term in equation (3.65) as follows,

$$(\nabla(\Delta\overline{\boldsymbol{v}}), \nabla(\Delta\overline{\boldsymbol{v}})) = \|\nabla(\Delta\overline{\boldsymbol{v}})\|^2 \geq \frac{1}{C_\delta}\|\Delta\overline{\boldsymbol{v}}\|^2 \geq \frac{1}{C_\delta^2}\|\nabla\overline{\boldsymbol{v}}\|^2. \tag{3.69}$$

We can insert (3.68) and (3.69) into (3.65) to get the following inequality

$$\begin{aligned}
\overline{q(\boldsymbol{v})} &= \frac{1}{4}\left(\overline{(\nabla\overline{\boldsymbol{v}},\nabla\overline{\boldsymbol{v}})} - \frac{\delta^2}{12}\overline{(\nabla\overline{\boldsymbol{v}},\nabla(\Delta\overline{\boldsymbol{v}}))} + \left(\frac{\delta^2}{24}\right)^2\overline{(\nabla(\Delta\overline{\boldsymbol{v}}),\nabla(\Delta\overline{\boldsymbol{v}}))}\right)\\
&\geq \frac{1}{4}\left(\overline{\|\nabla\overline{\boldsymbol{v}}\|^2} + \frac{\delta^2}{12}\cdot\frac{1}{C_\delta}\overline{\|\nabla\overline{\boldsymbol{v}}\|^2} + \left(\frac{\delta^2}{24}\right)^2\frac{1}{C_\delta^2}\overline{\|\nabla\overline{\boldsymbol{v}}\|^2}\right)\\
&= \frac{1}{4}\left(1 + \frac{\delta^2}{12}\cdot\frac{1}{C_\delta} + \left(\frac{\delta^2}{24}\right)^2\frac{1}{C_\delta^2}\right)\overline{\|\nabla\overline{\boldsymbol{v}}\|^2}\\
&= \frac{1}{4}\left(1 + \frac{\delta^2}{24}\cdot\frac{1}{C_\delta}\right)^2\overline{\|\nabla\overline{\boldsymbol{v}}\|^2}\\
&= c^2\overline{q(\overline{\boldsymbol{v}})}.
\end{aligned} \tag{3.70}$$

We can derive an estimation of $\overline{q(\boldsymbol{v})}$ using the inequality above, with $c = 1 + \pi^2/24$, as follows,

$$\overline{q(\boldsymbol{v})} \geq c^2\overline{q(\overline{\boldsymbol{v}})} \approx c^2 q(\overline{\boldsymbol{v}}).$$

On the other hand, we can take the consideration of the idealized situation of homogeneous, isotropic turbulence. It suggests that

$$\frac{|\overline{r(\boldsymbol{v})}|}{\left(\overline{q(\boldsymbol{v})}\right)^{3/2}} \approx \frac{|r(\overline{\boldsymbol{v}})|}{(q(\overline{\boldsymbol{v}}))^{3/2}}.$$

Inserting the two relations above leads to

$$\begin{aligned}
\nu_e &= C_\delta\frac{|\overline{r(\boldsymbol{v})}|}{\left(\overline{q(\boldsymbol{v})}\right)^{3/2}}\left(\overline{q(\boldsymbol{v})}\right)^{1/2}\\
&\approx \frac{|r(\overline{\boldsymbol{v}})|}{(q(\overline{\boldsymbol{v}}))^{3/2}}\left(\overline{q(\boldsymbol{v})}\right)^{1/2}\\
&\gtrsim C_\delta\frac{|\overline{r(\boldsymbol{v})}|}{(q(\overline{\boldsymbol{v}}))^{3/2}}\cdot c\,(q(\overline{\boldsymbol{v}}))^{1/2}\\
&= c\,C_\delta\frac{|r(\overline{\boldsymbol{v}})|}{q(\overline{\boldsymbol{v}})}\\
&\gtrsim c\,C_\delta\frac{|r(\boldsymbol{v})|}{q(\boldsymbol{v})}.
\end{aligned} \tag{3.71}$$

The last inequality was derived from the approximation $q(\overline{\boldsymbol{v}}) = q(\boldsymbol{v}) + O(\delta^2)$, and $r(\overline{\boldsymbol{v}}) = r(\boldsymbol{v}) + O(\delta^2)$. Therefore, we can reformulation the Navier-Stokes equation using the Verstappen model to have

$$\partial_t\boldsymbol{v} - \nabla\cdot\left(\left(2\nu + 2c\,C_\delta\frac{|r(\boldsymbol{v})|}{q(\boldsymbol{v})}\|\mathbb{D}(\boldsymbol{v})\|\right)\mathbb{D}(\boldsymbol{v})\right) + (\boldsymbol{v}\cdot\nabla)\boldsymbol{v} + \nabla r = \boldsymbol{f}. \tag{3.72}$$

Now we need to look into the eddy viscosity model in (3.72). Since the constant $c = 1 + \pi^2/24$. According to [7], we will approximate it as $c = 3/2$. And as defined in (3.37), we have C_δ depends on δ. In the paper of [7], the mesh scale $\delta = C_{FW} \cdot h_K$ is used for the numerical study later on, where $C_{FW} \cdot h_K$ is the local filter width, and h_K is the length of the shortest edge of the mesh cell K. Therefore, we can derive the eddy viscosity model in the Verstappen model as follows,

$$\begin{aligned}
\nu_e &= 2c\, C_\delta \frac{|r(\boldsymbol{v})|}{q(\boldsymbol{v})} \\
&= 2 \cdot \frac{3}{2} \cdot \left(\frac{C_{FW} \cdot h_K}{\pi} \right)^2 \frac{|-\det \mathbb{D}(\boldsymbol{v})|}{\frac{1}{2}\|\mathbb{D}(\boldsymbol{v})\|_F^2} \\
&= 6 \left(\frac{C_{FW} \cdot h_K}{\pi} \right)^2 \frac{|\det \mathbb{D}(\boldsymbol{v})|}{\|\mathbb{D}(\boldsymbol{v})\|_F^2}.
\end{aligned}$$

In the numerical study, we would choose the value of C_{FW} to find the most suitable parameter of the Verstappen model.

4 The Variational Multiscale Method

The variational multiscale method is applied for simulating the large flow structures. The large scales will be defined differently as in the large eddy simulation. We consider the large scales in the large eddy simulation as a space averaging filtering results. However, in the variational multiscale method, we define the large scales by projection into appropriate spaces.

4.1 The definition of the VMS method

Suppose we have the Navier-Stokes equation as in (2.12), and we consider that it has homogeneous Dirichlet boundary conditions. The idea of VMS method is to decompose the flow into three scales, which is, the large scales $(\overline{\boldsymbol{u}}, \overline{p})$, the resolved small scales $(\tilde{\boldsymbol{u}}, \tilde{p})$ and the unresolved small scales $(\hat{\boldsymbol{v}}, \hat{p})$. And we have $\boldsymbol{u} = \overline{\boldsymbol{u}} + \tilde{\boldsymbol{u}} + \hat{\boldsymbol{u}}$, $p = \overline{p} + \tilde{p} + \hat{p}$. We define the field $(\boldsymbol{v}, q) \in V \times Q$, where $V = (H_0^1(\Omega))^d$ under the norm $\|\boldsymbol{v}\|_V = \|\nabla \boldsymbol{v}\|_{L^2}$, and $Q = L_0^2(\Omega)$. Hence, the variational formulation of (12) can be written as follows:

Find $(\boldsymbol{u}, p) : (0, T] \to V \times Q$, such that for all $(\boldsymbol{v}, q) \in V \times Q$, the equation holds:

$$\begin{aligned} (\boldsymbol{u}_t, \boldsymbol{v}) + (2\mathrm{Re}^{-1}\mathbb{D}(\boldsymbol{u}), \mathbb{D}(\boldsymbol{v})) + b(\boldsymbol{u}, \boldsymbol{u}, \boldsymbol{v}) - (p, \nabla \cdot \boldsymbol{v}) + (q, \nabla \cdot \boldsymbol{u}) &= (\boldsymbol{f}, \boldsymbol{v}) \\ \boldsymbol{u}(0, \boldsymbol{x}) &= \boldsymbol{u}_0(\boldsymbol{x}), \end{aligned} \tag{4.1}$$

where $b(\boldsymbol{u}, \boldsymbol{v}, \boldsymbol{w}) = ((\boldsymbol{u} \cdot \nabla)\boldsymbol{v}, \boldsymbol{w})$.

To be convenience, we replace the long equation (4.1) with a short form as follows:

$$A(\boldsymbol{u}; (\boldsymbol{u}, p), (\boldsymbol{v}, q)) = F(\boldsymbol{v}). \tag{4.2}$$

We can now decompose the test functions into the three scales as we defined before. Then we get a coupled system, which is, finding the right decomposition of $(\boldsymbol{u}, p)$, and applying the linearity of the variational problem with respect to the test function. We have:

$$\begin{aligned} A(\boldsymbol{u}; (\overline{\boldsymbol{u}}, \overline{p}), (\overline{\boldsymbol{v}}, \overline{q})) + A(\boldsymbol{u}; (\tilde{\boldsymbol{u}}, \tilde{p}), (\overline{\boldsymbol{v}}, \overline{q})) + A(\boldsymbol{u}; (\hat{\boldsymbol{u}}, \hat{p}), (\overline{\boldsymbol{v}}, \overline{q})) &= F(\overline{\boldsymbol{v}}), \\ A(\boldsymbol{u}; (\overline{\boldsymbol{u}}, \overline{p}), (\tilde{\boldsymbol{v}}, \tilde{q})) + A(\boldsymbol{u}; (\tilde{\boldsymbol{u}}, \tilde{p}), (\tilde{\boldsymbol{v}}, \tilde{q})) + A(\boldsymbol{u}; (\hat{\boldsymbol{u}}, \hat{p}), (\tilde{\boldsymbol{v}}, \tilde{q})) &= F(\tilde{\boldsymbol{v}}), \\ A(\boldsymbol{u}; (\overline{\boldsymbol{u}}, \overline{p}), (\hat{\boldsymbol{v}}, \hat{q})) + A(\boldsymbol{u}; (\tilde{\boldsymbol{u}}, \tilde{p}), (\hat{\boldsymbol{v}}, \hat{q})) + A(\boldsymbol{u}; (\hat{\boldsymbol{u}}, \hat{p}), (\hat{\boldsymbol{v}}, \hat{q})) &= F(\hat{\boldsymbol{v}}). \end{aligned} \tag{4.3}$$

We can consider more about the form of the coupled system. The basic idea of the VMS method is to neglect the equation with test function $(\hat{\boldsymbol{v}}, \hat{q})$ at first. Then we assume that the unresolved scales have no influence on the large scales directly. The influence of the unresolved scales onto the small resolved scales is described in

$$A(\boldsymbol{u}; (\hat{\boldsymbol{u}}, \hat{p}), (\tilde{\boldsymbol{v}}, \tilde{q})) \approx B(\boldsymbol{u}; (\overline{\boldsymbol{u}}, \overline{p}), (\tilde{\boldsymbol{u}}, \tilde{p}), (\tilde{\boldsymbol{v}}, \tilde{q})). \tag{4.4}$$

Let $\overline{V}$ and $\overline{Q}$ be the spaces that representing the solution fields of large scales and its corresponding test function fields. And let $\tilde{V}$ and $\tilde{Q}$ be the solution field for the resolved small scales. We can get a new form of equations after neglecting the unresolved scales and inserting the turbulence model B as follows:

Find $(\overline{\boldsymbol{u}}, \tilde{\boldsymbol{u}}, \overline{p}, \tilde{p}) \in \overline{V} \times \tilde{V} \times \overline{Q} \times \tilde{Q}$, such that the equations hold,

$$\begin{aligned} A(\overline{\boldsymbol{u}} + \tilde{\boldsymbol{u}}; (\overline{\boldsymbol{u}}, \overline{p}), (\overline{\boldsymbol{v}}, \overline{q})) + A(\overline{\boldsymbol{u}} + \tilde{\boldsymbol{u}}; (\tilde{\boldsymbol{u}}, \tilde{p}), (\overline{\boldsymbol{v}}, \overline{q})) &= F(\overline{\boldsymbol{v}}), \\ A(\overline{\boldsymbol{u}} + \tilde{\boldsymbol{u}}; (\overline{\boldsymbol{u}}, \overline{p}), (\tilde{\boldsymbol{v}}, \tilde{q})) + A(\overline{\boldsymbol{u}} + \tilde{\boldsymbol{u}}; (\tilde{\boldsymbol{u}}, \tilde{p}), (\tilde{\boldsymbol{v}}, \tilde{q})) + & \\ B(\overline{\boldsymbol{u}} + \tilde{\boldsymbol{u}}; (\overline{\boldsymbol{u}}, \overline{p}), (\tilde{\boldsymbol{u}}, \tilde{p}), (\tilde{\boldsymbol{v}}, \tilde{q})) &= F(\tilde{\boldsymbol{v}}). \end{aligned} \tag{4.5}$$

4.2 A three-scale coarse space projection-based VMS method

Suppose we have finite element spaces for the velocity and pressure $V^h \times Q^h$. And L^H is a finite-dimensional space of symmetric $d \times d$ tensor-valued functions on Ω. We define $\nu_T((\boldsymbol{w}^h, \boldsymbol{r}^h), h)$ to be a non-negative function. Hence, the semi-discrete coarse space projection-based VMS method is defined as follows:

Find $\boldsymbol{w}^h : (0, T] \to V^h$, $\boldsymbol{r}^h : (0, T] \to Q^h$, and $\mathbb{G}^H : (0, T] \to L^H$, such that for all $(\boldsymbol{v}^h, q^h) \in v^H \times Q^h$ and $\mathbb{L}^H \in L^H$, it satisfies

$$\begin{aligned} (\partial_t \boldsymbol{w}^h, \boldsymbol{v}^h) + (2\nu \mathbb{D}(\boldsymbol{w}^h), \mathbb{D}(\boldsymbol{v}^h)) + n(\boldsymbol{w}^h, \boldsymbol{w}^h, \boldsymbol{v}^h) & \\ -(\nabla \cdot \boldsymbol{v}^h, \boldsymbol{r}^h) + (\nu_T(\mathbb{D}(\boldsymbol{w}^h) - \mathbb{G}^H), \mathbb{D}(\boldsymbol{v}^h)) &= \langle \boldsymbol{f}, \boldsymbol{v}^h \rangle_{V',V}, \\ (\nabla \cdot \boldsymbol{w}^h, q^h) &= 0, \\ (\mathbb{D}(\boldsymbol{w}^h) - \mathbb{G}^H, \mathbb{L}^H) &= 0. \end{aligned} \tag{4.6}$$

The last equation in (4.6) defines large scales and small resolved scales. The choice of ν_T is mentioned in Chapter 3 as equation (3.21). The tensor $\mathbb{G}^H$ is the $L^2(\Omega)$ projection of $\mathbb{D}(\boldsymbol{w}^h)$ into L^H , i.e.,

$$\begin{aligned} P_{L^H} : L = \mathbb{D}(V) &\to L^H, \\ \mathbb{D}(\boldsymbol{v}) &\mapsto P_{L^H} \mathbb{D}(\boldsymbol{v}) = \mathbb{G}^H. \end{aligned} \tag{4.7}$$

Therefore, we have the following formulation,

$$(P_{L^H} \mathbb{D}(\boldsymbol{v}) - \mathbb{D}(\boldsymbol{v}), \mathbb{L}^H) = 0, \qquad \forall \mathbb{L}^H \in L^H. \tag{4.8}$$

We can apply the short form as in (4.2) and (4.8) to reformulate the first equation of (4.6) as follows:

Find $\boldsymbol{w}^h : (0, T] \to V^h$, $\boldsymbol{r}^h : (0, T] \to Q^h$, such that for all $(\boldsymbol{v}^h, q^h) \in V^h \times Q^h$, it satisfies

$$A(\boldsymbol{w}^h; (\boldsymbol{w}^h, \boldsymbol{r}^h), (\boldsymbol{v}^h, q^h)) + (\nu_T(I - P_{L^H})\mathbb{D}(\boldsymbol{w}^h), \mathbb{D}(\boldsymbol{v}^h)) = \langle \boldsymbol{f}, \boldsymbol{v}^h \rangle_{V',V}. \tag{4.9}$$

Since L^H is a space of large scales, $(I - P_{L^H})\mathbb{D}(\boldsymbol{w}^h)$ represents small resolved scales of $\mathbb{D}(\boldsymbol{w}^h)$. We define that $L^H \subset \mathbb{D}(\boldsymbol{v}^h) \in V^h$ to avoid a negative additional viscosity.

If V^h is a higher order finite element space, then L^H can be defined as a low order finite element space applying the same grid as in V^h. If V^h is a low order finite element space, then L^H can be defined as applying a coarser grid. Since $\mathbb{D}(\boldsymbol{w}^h)$ is defined as a discontinuous piecewise polynomial tensor in V^h, L^H should be defined as a projection in the same way, consisting of discontinuous piecewise polynomial tensors.

5 Numerical Studies

5.1 An example for turbulent flow problems

We have a turbulent channel flow problem which is governed by the dimensionless incompressible Navier-Stokes equations as in equation (2.12). We want to set the parameters of the dimensionless incompressible Navier-Stokes equations to be $L = 1m$, $U = 1m/s$. And we notice that the dimensionless viscosity is exactly $\mathrm{Re}^{-1} = \nu = \mathrm{Re}_\tau^{-1} m^2/s$.

We take an example of the turbulent channel flow at $\mathrm{Re}_\tau = 395$ and $\mathrm{Re}_\tau = 590$ in our study. Therefore the difference between the two examples is only in the value of ν. The choice of Reynolds number based on the channel half width, the kinematic viscosity ν and the friction velocity U_τ. We define here the channel half width $H = 1$. Then the problem is given in

$$\Omega = (-\pi, \pi) \times (0, 2) \times (-\frac{\pi}{2}, \frac{\pi}{2}). \tag{5.1}$$

For the consideration of boundary condition, we define with no-slip conditions $\boldsymbol{u} = \mathbf{0}$ at solid walls along the y-direction at $y = 0$ and $y = 2$. Along the x-axis and z-axis the boundary conditions are periodically defined. We use the mean velocity as the definition of an initial condition $U_{\mathrm{mean}}(y)$. The data is imported from Gravemeier (2006b) as follows,

$$\begin{aligned} \boldsymbol{u}_1(0; x, y, z) &= U_{\mathrm{mean}}(y) + 0.1 U_{\mathrm{bulk}} \psi(x, y, z), \\ \boldsymbol{u}_2(0; x, y, z) &= 0.1 U_{\mathrm{bulk}} \psi(x, y, z), \\ \boldsymbol{u}_3(0; x, y, z) &= 0.1 U_{\mathrm{bulk}} \psi(x, y, z), \end{aligned} \tag{5.2}$$

where,

$$U_{\mathrm{bulk}} = \frac{1}{H} \int_0^H U_{\mathrm{mean}}(y) dy \approx 15.6803. \tag{5.3}$$

The initial velocity field (5.1) is obtained by a random velocity fluctuation around the mean velocity profile. We set the fluctuation field to be $\pm 10\%$ of the bulk velocity. And $\psi(x, y, z)$ is noise with a random function of the form as follows,

$$\psi(x, y, z) = \frac{2\,\mathrm{rand}()}{\mathrm{RAND\_MAX}()} - 1 \in [-1, 1]. \tag{5.4}$$

With the reference of Moser et al, the bulk velocity is defined as $U_{\mathrm{bulk}} = 17.5452$. And the initial velocity field can be defined in the same way as in (5.1).

For the results of the calculation of the examples, we are interested in the mean velocity and the Reynolds stresses. We use the following equations to compute the arithmetic

mean of the velocity field and the spatial average

$$\begin{aligned}\langle \boldsymbol{u}^h(t,\boldsymbol{x})\rangle_t &= \frac{1}{N_t+1}\sum_{n=0}^{N_t}\boldsymbol{u}^h(t_n,\boldsymbol{x}),\\ \langle \boldsymbol{u}^h(t_n,x,y,z)\rangle_s &= \frac{1}{N_x}\frac{1}{N_z}\sum_{i=1}^{N_x}\sum_{j=1}^{N_z}\boldsymbol{u}^h(t_n,x_i,y,z_j),\end{aligned} \tag{5.5}$$

where N_t denotes the number of time steps, N_x and N_z are the numbers of degrees of freedom in the x-axis and z-axis.

Therefore, we can derive the first order quantity of the mean velocity as follows,

$$\boldsymbol{u}^h_{\text{mean}}(y) = \langle\langle \boldsymbol{u}^h(t_n,x,y,z)\rangle_s\rangle_t. \tag{5.6}$$

For the other quantity of interest, the Reynolds stresses , we use the definition of the Reynolds stress tensor to have,

$$\mathbb{T}^h_{ij,\text{mean}} = \langle\langle u^h_i u^h_j\rangle_s\rangle_t - \langle\langle u^h_i\rangle_s\rangle_t\langle\langle u^h_j\rangle_s\rangle_t, \qquad i,j=1,2,3. \tag{5.7}$$

The Reynolds stress is not uniquely defined in the literature. In the paper of [8], it is explained that the diagonal Reynolds stresses computed with the solution of turbulent flow simulations cannot be compared with the diagonal stresses of the turbulent flow field. Only the so-called root mean squared turbulence, which is defined below, can be studied directly

$$\boldsymbol{u}^h_{i,\text{rms}} = \left|\mathbb{T}^h_{ii,\text{mean}} - \frac{1}{3}\sum_{j=1}^{3}\mathbb{T}^h_{jj,\text{mean}}\right|^{1/2}, \qquad i=1,2,3. \tag{5.8}$$

5.2 Experiment results

The experiments are performed with the code ParMooN. We define the finite element method (FEM) space for the velocity is continuous quadratic polynomials on hexahedra, and for the pressure is discontinuous linear polynomials on hexahedra. We apply Crank-Nilson method for the temporal derivation. The time step is 0.002 and the time interval is defined to be $[0, 40]$. In the experiments, the degree of freedom for the velocity is $3 \cdot 66\,560$, and for the pressure is $32\,768$.

The purpose of the experiments is to select the best constant of the model, which fits the example that we discussed in the last section. We have set two different values of the parameter Re_τ for the experiment. The first one we performed is $\text{Re}_\tau = 395$, and the second one is $\text{Re}_\tau = 590$. In the same time, three eddy viscosity models for the VMS method (4.6) are considered in this experiment, the Smagorinsky model, the Smagorinsky model with van Driest damping, and the Verstappen model.

We want to find for each of the models above a most suitable constant. Therefore, we apply for each model different constants in order to see which, among the constants, gives us the best result. In the last step, we would compare the three models with their best fits results, in order to give the best simulation under the situation.

5.2.1 Experiments with $\mathrm{Re}_\tau = 395$

Firstly, we consider the experiment under the setting of $\mathrm{Re}_\tau = 395$. We define the parameters, which is varied in the Smagorinsky model and the Smagorinsky van Driest model (short for the Smagorinsky model with van Driest Damping), to be the turbulent viscosity constant. And for the first round calculation, we set them to be 0.005, 0.0075, 0.01, 0.015, and 0.02. The results of the calculation will be written into a data file ended with ".out". We use python to analyse the results in comparison to the benchmark data, which is referred to as "reference curve" in the final figures.

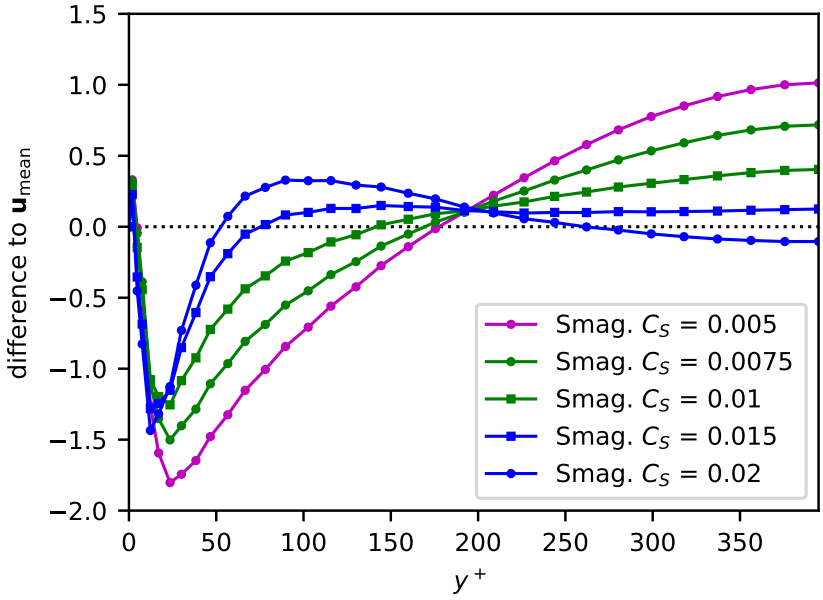

(a) Smagorinsky model with $C_S = 0.005$, 0.0075, 0.01, 0.015 and 0.02.

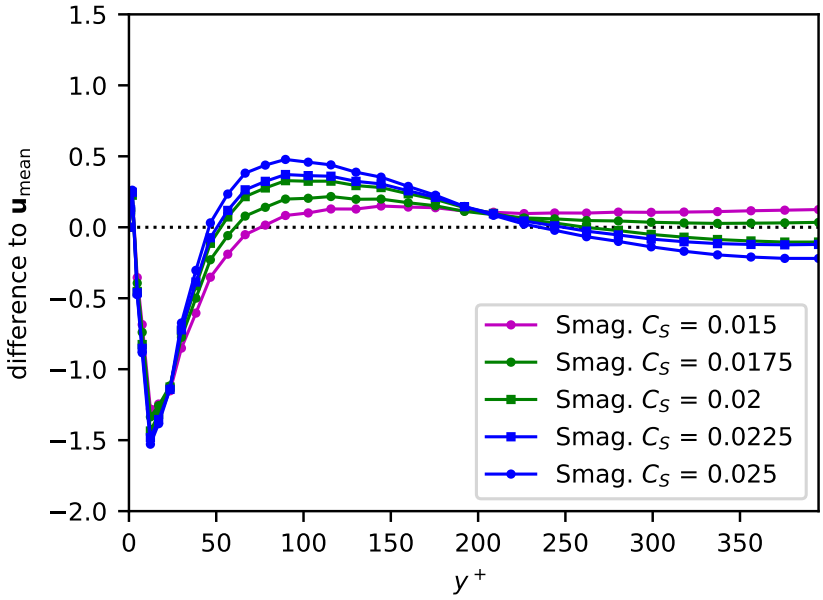

(b) Smagorinsky model with $C_S = 0.015$, 0.0175, 0.02, 0.0225 and 0.025.

Figure 5.1: $\mathrm{Re}_\tau = 395$, Smagorinsky model: Comparison between turbulent viscosity constants in difference to the mean.

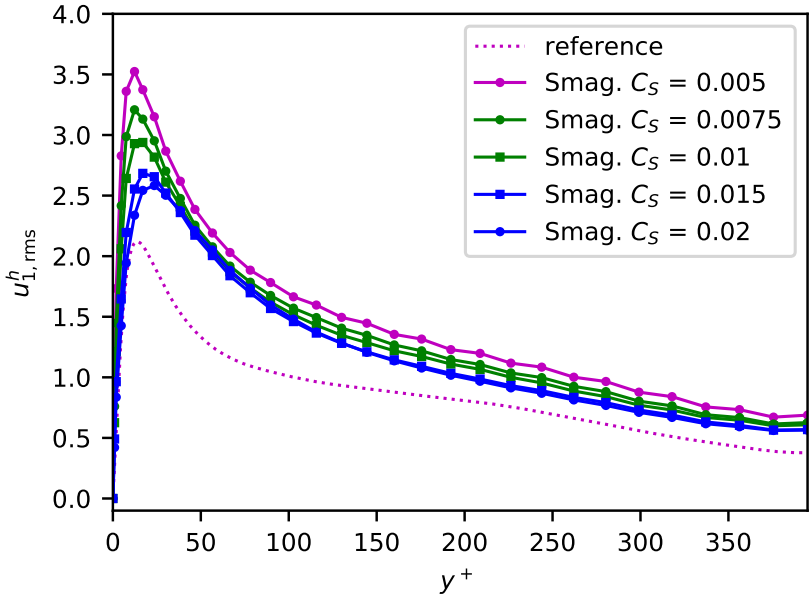

(a) Smagorinsky model with $C_S = 0.005$, 0.0075, 0.01, 0.015 and 0.02.

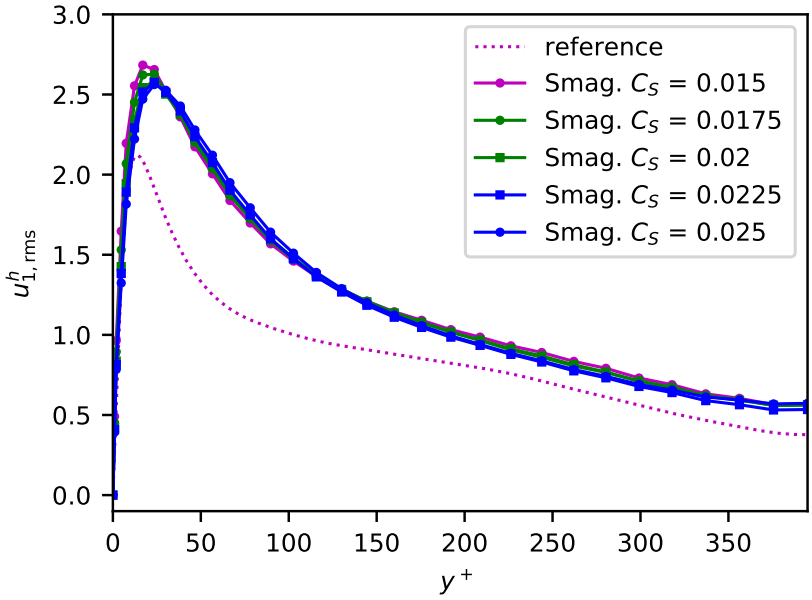

(b) Smagorinsky model with $C_S = 0.015$, 0.0175, 0.02, 0.0225 and 0.025.

Figure 5.2: $\mathrm{Re}_\tau = 395$, Smagorinsky model: Comparison between turbulent viscosity constants in Root Mean Squared tensor

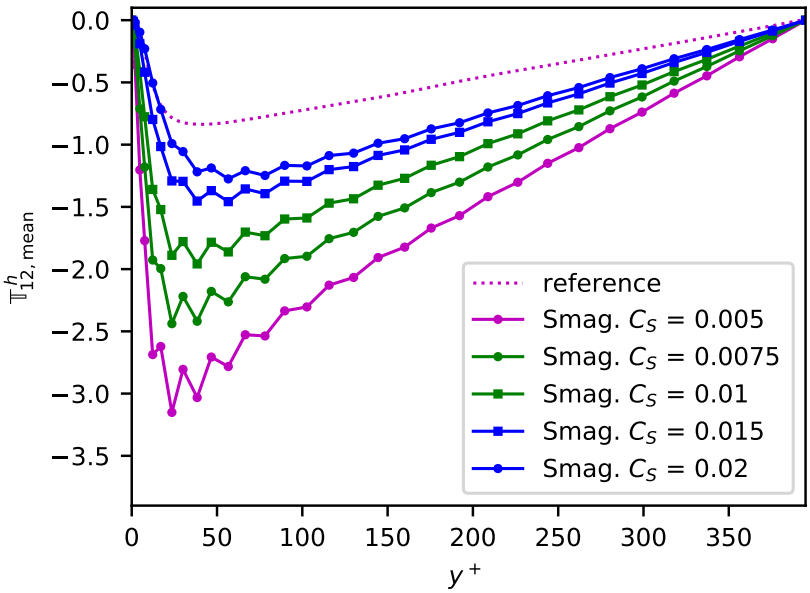

(a) Smagorinsky model with $C_S = 0.005$, 0.0075, 0.01, 0.015 and 0.02.

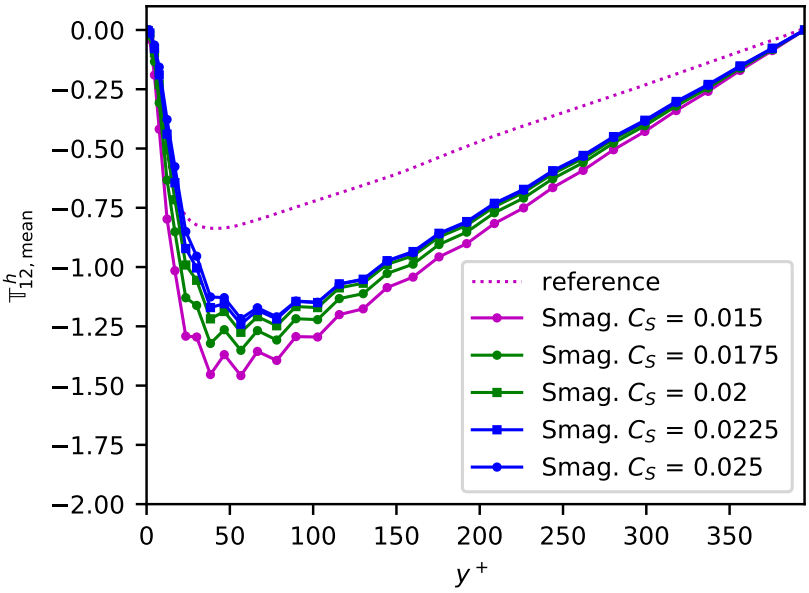

(b) Smagorinsky model with $C_S = 0.015$, 0.0175, 0.02, 0.0225 and 0.025.

Figure 5.3: $\mathrm{Re}_\tau = 395$, Smagorinsky model: Comparison between turbulent viscosity constants in Reynolds Stress tensor.

After comparing the first round results, we observe that, from Figure 5.1(a), Figure 5.2(a) and Figure 5.3(a), the curves of value equals to 0.015 and 0.02 are the nearest to the reference curve. Thus we select some values that around the two values and repeat the code. We have chosen the new group of the turbulent viscosity constants to be 0.015, 0.0175, 0.02, 0.0225, 0.025. And from Figure 5.1(b), Figure 5.2(b), and Figure 5.3(b), we observe that the second round calculation does not change much about the results. The curves go near to the reference curve, but the curves with value 0.02 behave belong always to the best ones. Therefore, for Smagorinsky model under the setting of $\mathrm{Re}_\tau = 395$, we choose the simulation which has the turbulent viscosity constant equals to 0.02, to be the best choice of the Smagorinsky model.

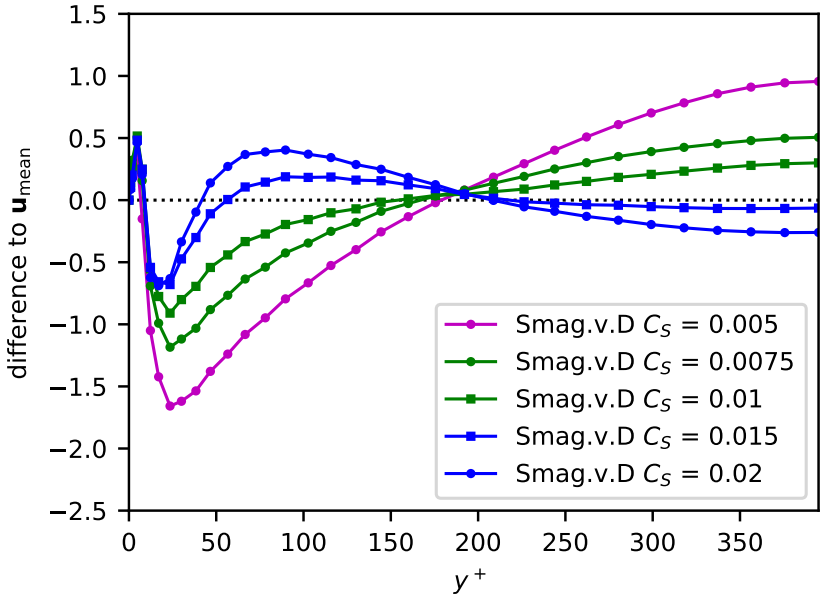

(a) Smagorinsky van Driest model with $C_S = 0.005$, 0.0075, 0.01, 0.015 and 0.02.

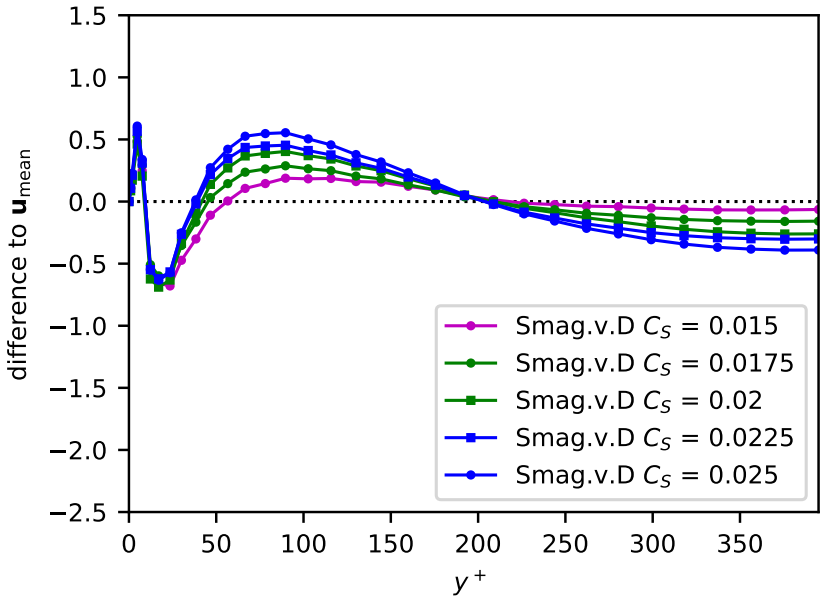

(b) Smagorinsky van Driest model with $C_S = 0.015$, 0.0175, 0.02, 0.0225 and 0.025.

Figure 5.4: $\text{Re}_\tau = 395$, Smagorinsky van Driest model: Comparison between turbulent viscosity constants in difference to the mean.

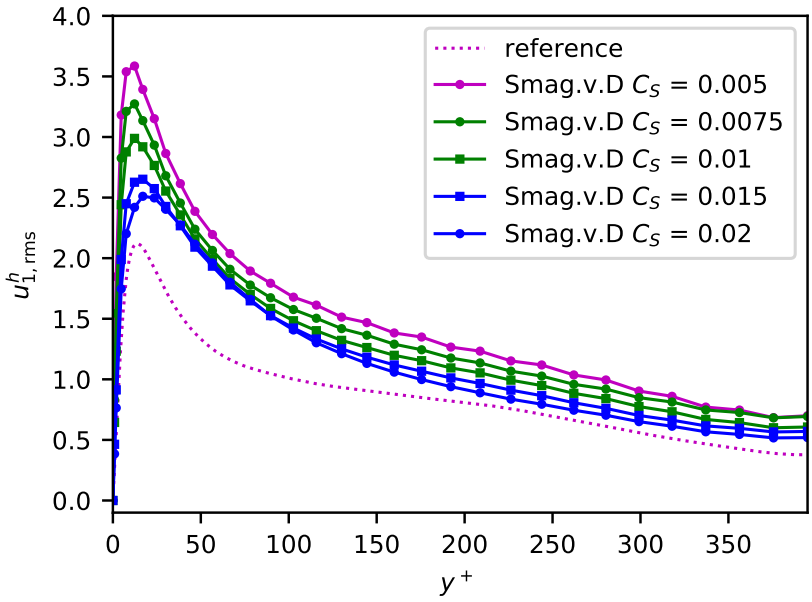

(a) Smagorinsky van Driest model with C_S = 0.005, 0.0075, 0.01, 0.015 and 0.02.

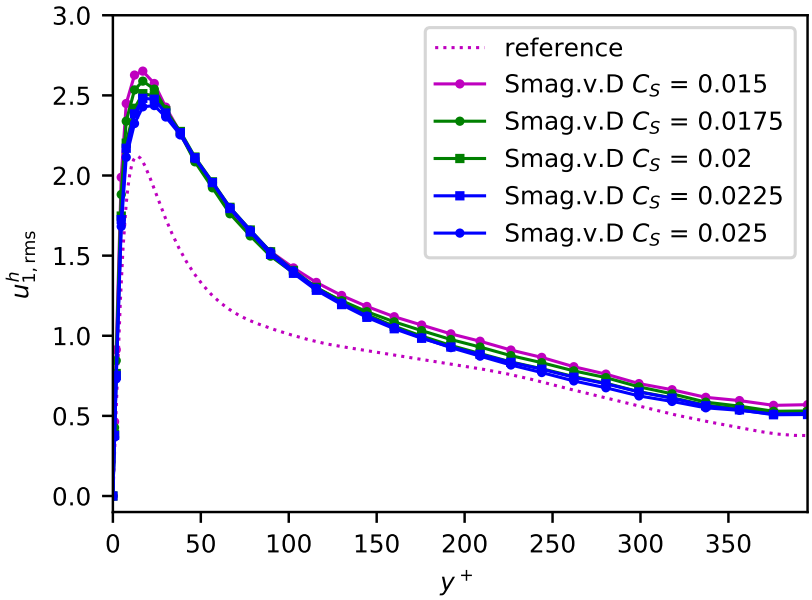

(b) Smagorinsky van Driest model with C_S = 0.015, 0.0175, 0.02, 0.0225 and 0.025.

Figure 5.5: Re_τ = 395, Smagorinsky van Driest model: Comparison between turbulent viscosity constants in Root Mean Squared tensor.

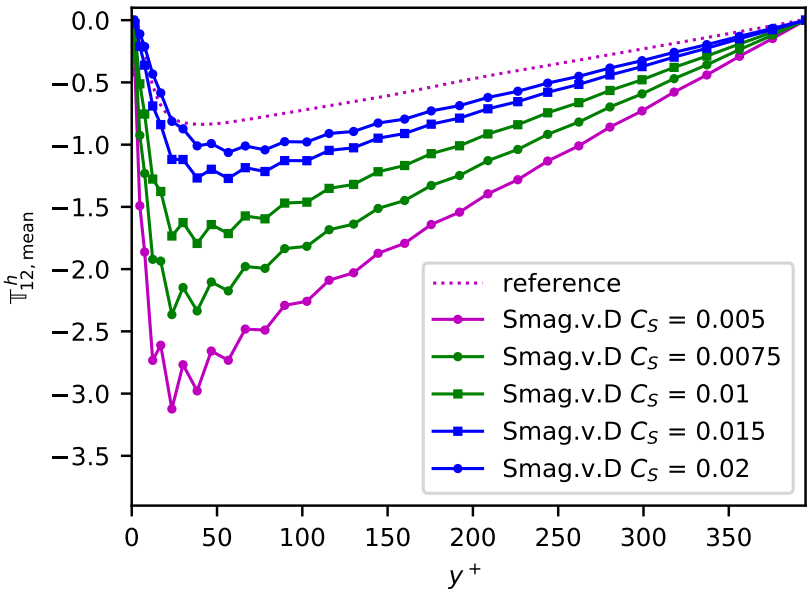

(a) Smagorinsky van Driest model with $C_S = 0.005$, 0.0075, 0.01, 0.015 and 0.02.

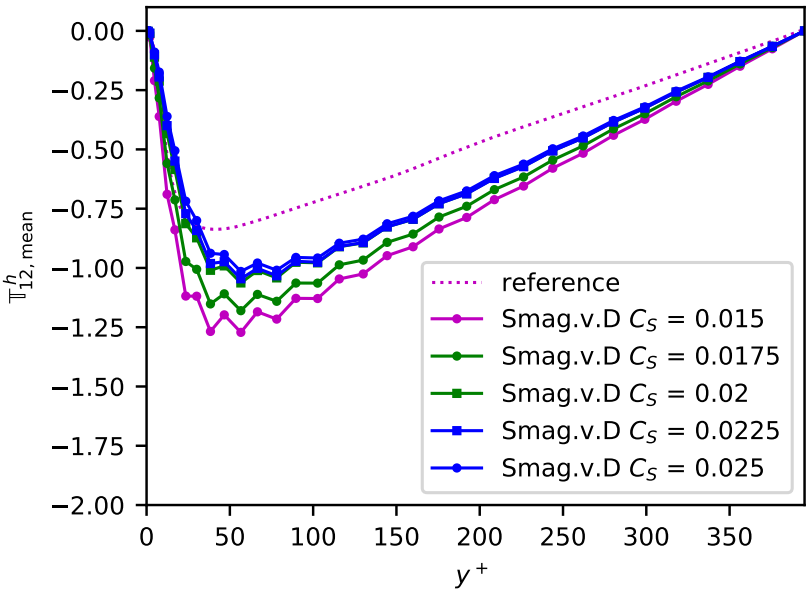

(b) Smagorinsky van Driest model with $C_S = 0.015$, 0.0175, 0.02, 0.0225 and 0.025.

Figure 5.6: $\mathrm{Re}_\tau = 395$, Smagorinsky van Driest model: Comparison between turbulent viscosity constants in Reynolds Stress tensor.

We repeat the same comparison with Smagorinsky model with van Driest Damping. From Figure 5.4(a), Figure 5.5(a), and Figure 5.6(a), we can see that the constant with value 0.015 and 0.02 behave good. Hence, we repeat the same code again with the new group of constants equal to 0.015, 0.0175, 0.02, 0.0225 and 0.025. From Figure 5.4(b), we can see that, the curves 0.015 and 0.0175 go near to the reference curve. However, in Figure 5.5(b), and Figure 5.6(b), the curves 0.015 and 0.0175 are clearly worse. To this point, we consider that the better behavior in 5.4(b) is more important than the worse behavior in 5.5(b) and 5.6(b). Therefore, the turbulent viscosity constant that equals to 0.0175 is our choice for the Smagorinsky model with van Driest Damping.

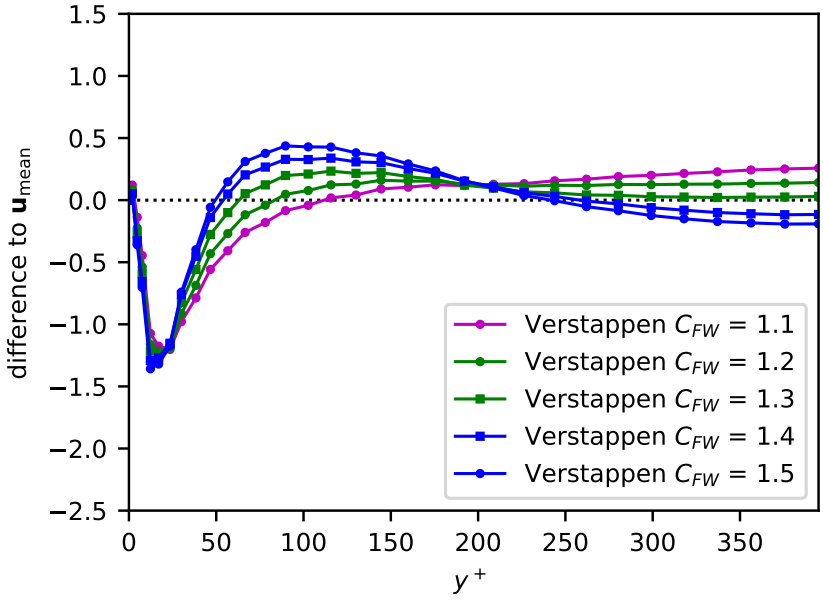

(a) Verstappen model with C_{FW} = 1.1, 1.2, 1.3, 1.4 and 1.5.

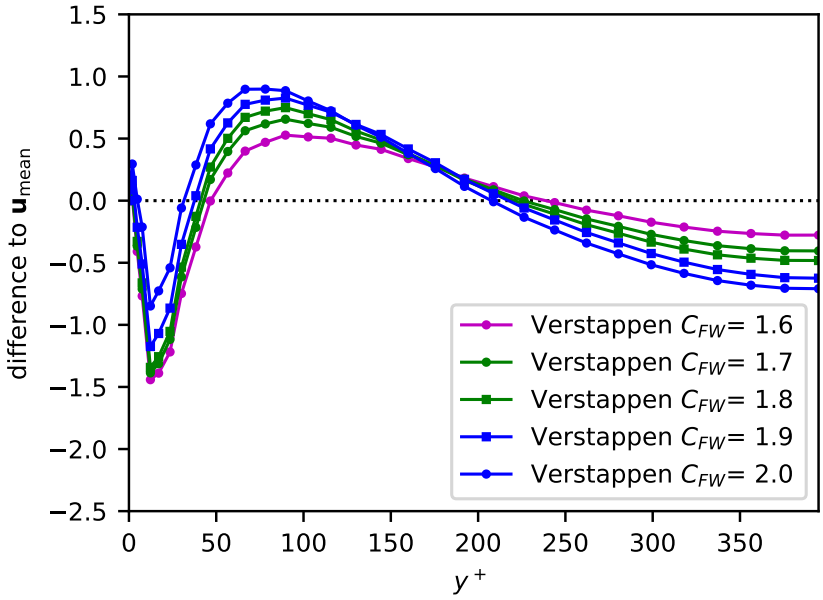

(b) Verstappen model with C_{FW} = 1.6, 1.7, 1.8, 1.9 and 2.0.

Figure 5.7: Re_τ = 395, Verstappen model: Comparison between filter width constants in difference to the mean.

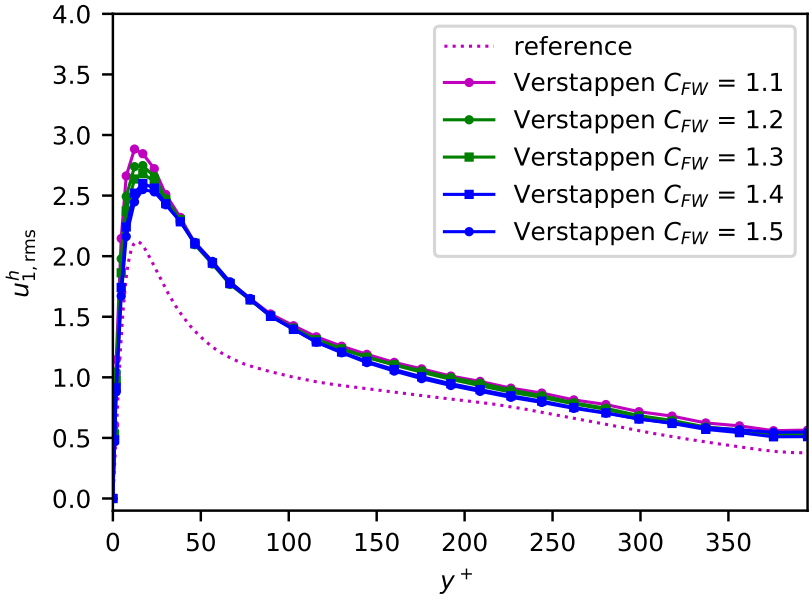

(a) Verstappen model with C_{FW} = 1.1, 1.2, 1.3, 1.4 and 1.5.

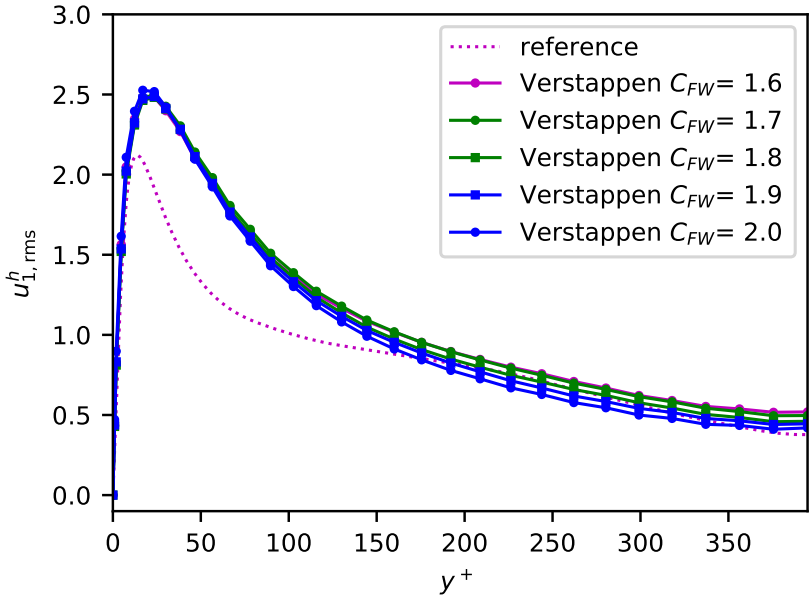

(b) Verstappen model with C_{FW} = 1.6, 1.7, 1.8, 1.9 and 2.0.

Figure 5.8: Re_τ = 395, Verstappen model: Comparison between filter width constants in Root Mean Square tensor.

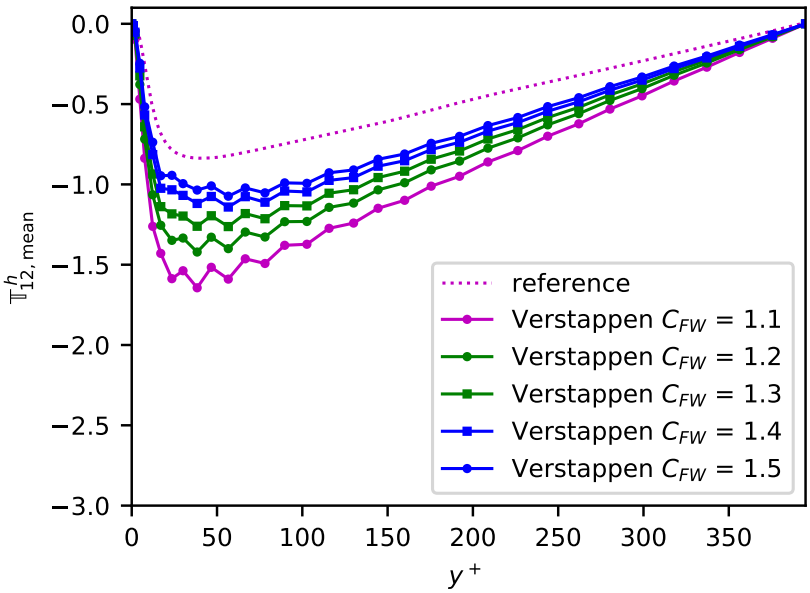

(a) Verstappen model with C_{FW} = 1.1, 1.2, 1.3, 1.4 and 1.5.

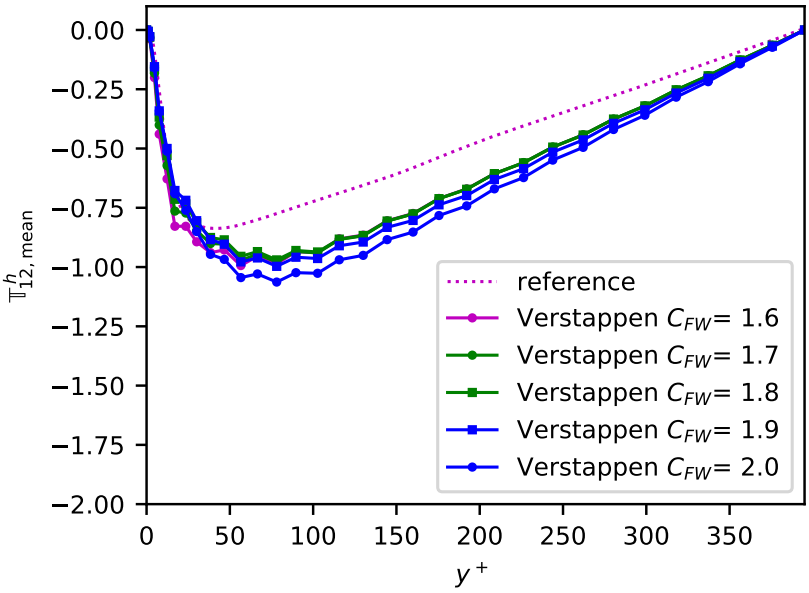

(b) Verstappen model with C_{FW} = 1.6, 1.7, 1.8, 1.9 and 2.0.

Figure 5.9: Re_τ = 395, Verstappen model: Comparison between filter width constants in Reynolds Stress tensor.

Now we look at the Verstappen model. The parameter that we change here is different, since the eddy viscosity parameter depends on the filter width Δ. We want to test what is the width that we can choose for the filter. Hence, the parameter that need to be varied in the Verstappen model is the filter width constant, in the range of $[1.0, 2.0]$. In Figure 5.7, we can see that the curve 1.1 is the nearest to the reference line, but it is much worse in Figure 5.8 and Figure 5.9. On the contrary, the curve 1.5 behaves really good in Figure 5.8 and Figure 5.9. And if we look back at Figure 5.7, we can see that the curve 1.5 is relatively good than all other curves. Hence, we can draw the conclusion that, based on the results, the curve 1.5 is a good compromise.

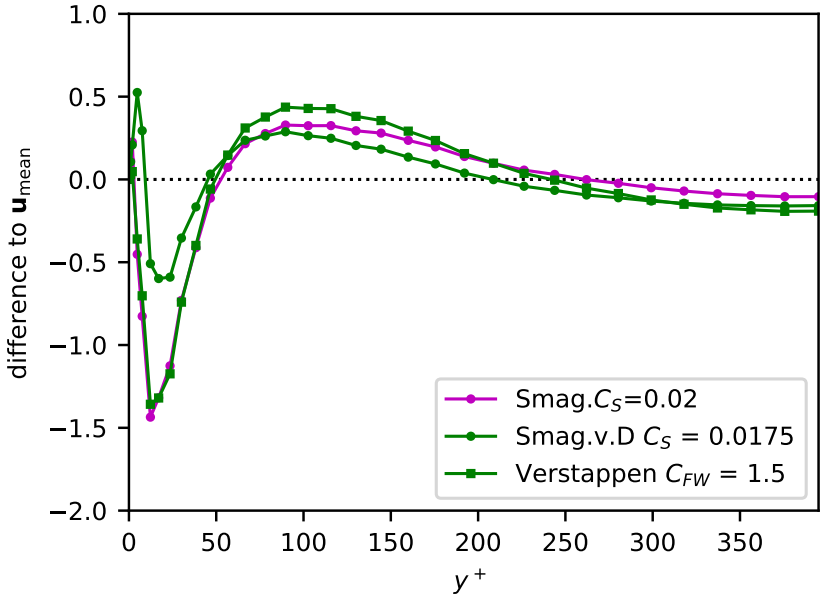

Figure 5.10: $\text{Re}_\tau = 395$, Comparison in difference to the mean.

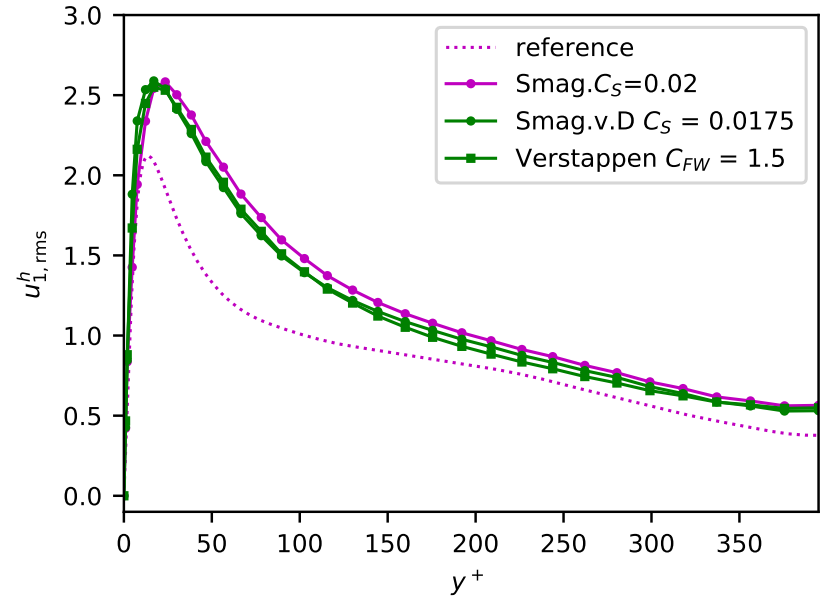

Figure 5.11: $\text{Re}_\tau = 395$, Comparison in Root Mean Squared tensor.

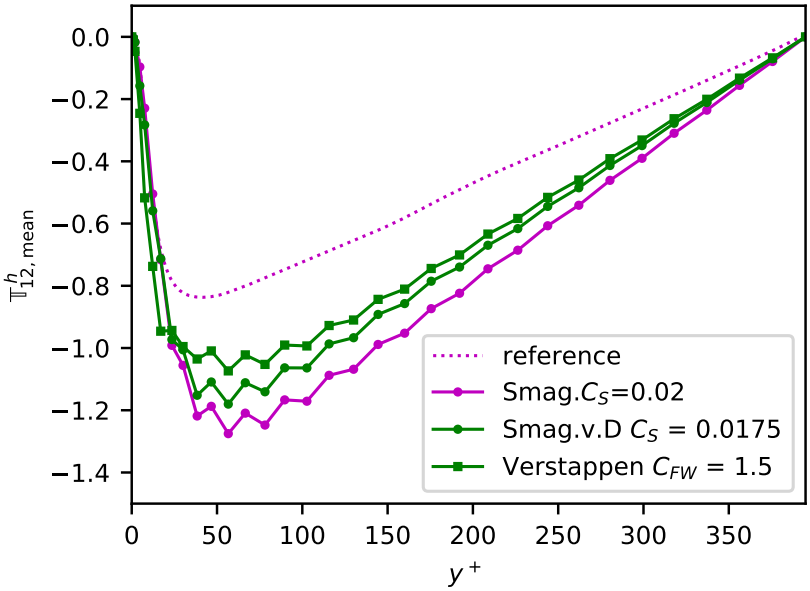

Figure 5.12: $\mathrm{Re}_\tau = 395$, Comparison in Reynolds Stress tensor.

The last step is to compare the curves between the three models. As we mentioned before, we choose Smagorinsky model with $C_S = 0.02$, Smagorinsky van Driest model with $C_S = 0.0175$ and Verstappen model with $C_{FW} = 1.5$. From Figure 5.10, the Smagorinsky model with van Driest Damping is better with respect to the quantity of interest "difference to the mean". On the other side, from Figure 5.12, the Verstappen model is better with respect to the quantity "Reynolds stress tensor". And for the quantity of interest "Root mean squared tensor", there are only minor differences according to Figure 5.11.

5.2.2 Experiments with $\mathrm{Re}_\tau = 590$

For the setting of $\mathrm{Re}_\tau = 590$, we repeat the same process as in the experiment of $\mathrm{Re}_\tau = 395$.

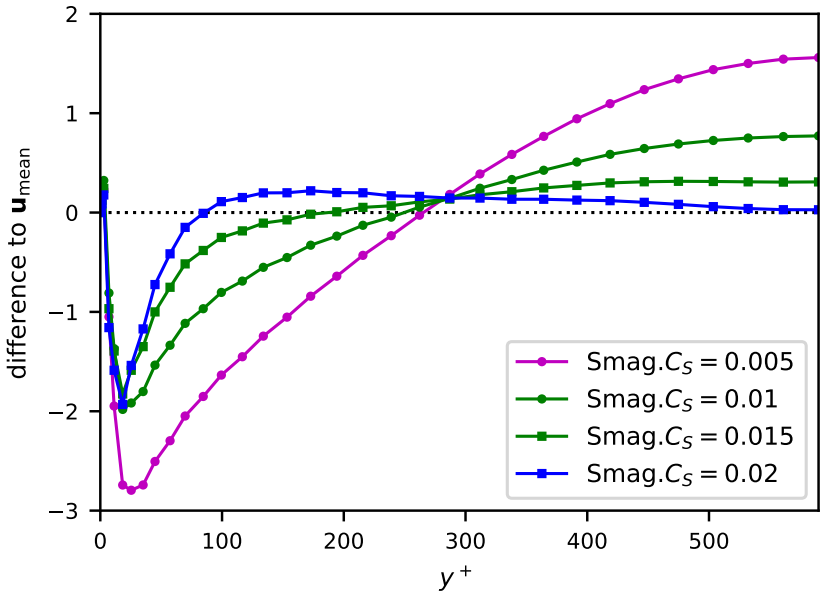

(a) Smagorinsky model with $C_S = 0.005$, 0.01, 0.015 and 0.02

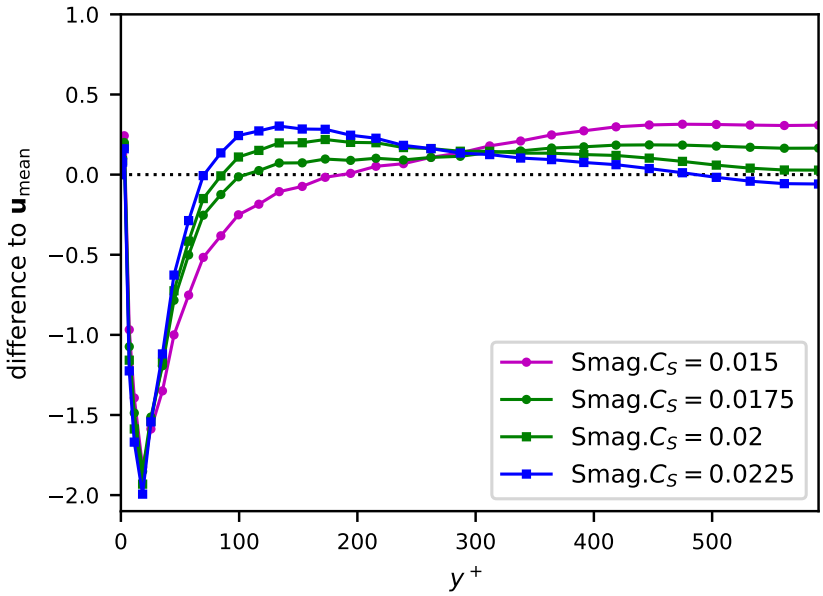

(b) Smagorinsky model with $C_S = 0.015$, 0.0175, 0.02 and 0.0225

Figure 5.13: $\mathrm{Re}_\tau = 590$, Smagorinsky model: Comparison between turbulent flow constant in difference to the mean.

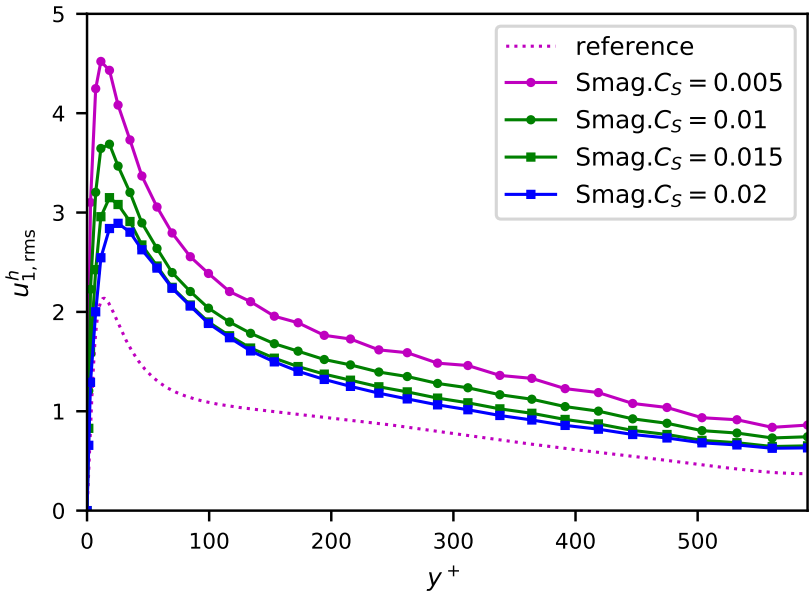

(a) Smagorinsky model with $C_S = 0.005$, 0.01, 0.015 and 0.02

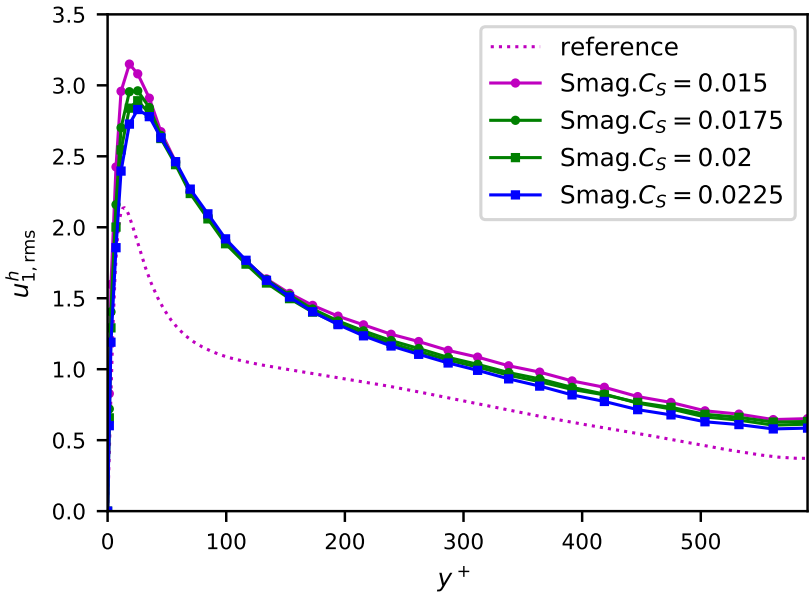

(b) Smagorinsky model with $C_S = 0.015$, 0.0175, 0.02 and 0.0225

Figure 5.14: $\mathrm{Re}_\tau = 590$, Smagorinsky model: Comparison between turbulent flow constant in Root Mean Square tensor.

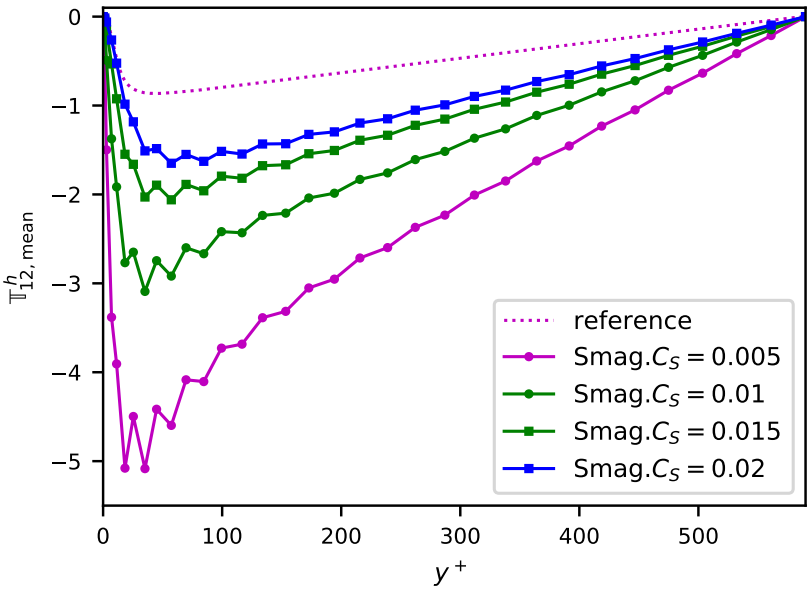

(a) Smagorinsky model with $C_S = 0.005$, 0.01, 0.015 and 0.02

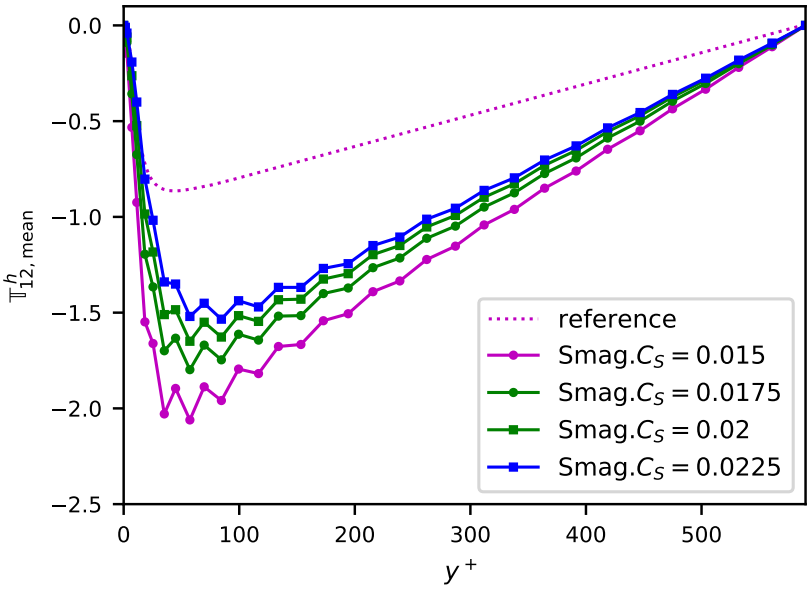

(b) Smagorinsky model with $C_S = 0.015$, 0.0175, 0.02 and 0.0225

Figure 5.15: $\mathrm{Re}_\tau = 590$, Smagorinsky model: Comparison between turbulent flow constant in Reynolds Stress tensor.

In the first round experiments, we have chosen for the Smagorinsky model the turbulent viscosity constants are the following constants: 0.005, 0.01, 0.015 and 0.02. We can see from Figure 5.13(a), Figure 5.14(a) and Figure 5.15(a) that the behaviors of the curves 0.005 and 0.01 are really bad. Hence, we dropped the constants 0.005 and 0.01, and add 0.0175 and 0.0225 to the second round experiments. From Figure 5.13(b), we can see that the curves 0.02 and 0.0225 are pretty good. Moreover, in both Figure 5.14(b) and Figure 5.15(b), we find out that the curve 0.0225 is indeed better than 0.02. Therefore, we would prefer to choosing 0.0225 as the best turbulent viscosity constant in the case $\mathrm{Re}_\tau = 590$ for the Smagorinsky model.

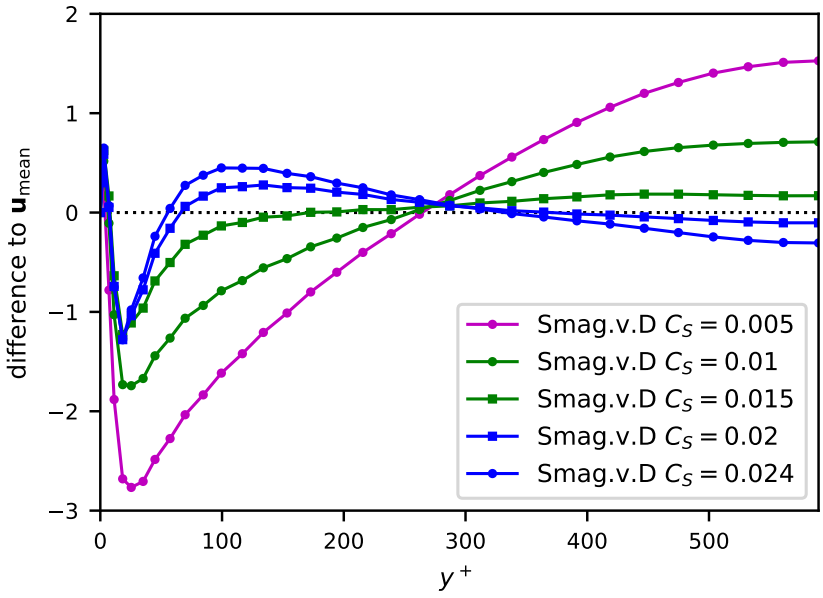

(a) Smagorinsky van Driest model with $C_S = 0.005$, 0.01, 0.015, 0.02 and 0.024

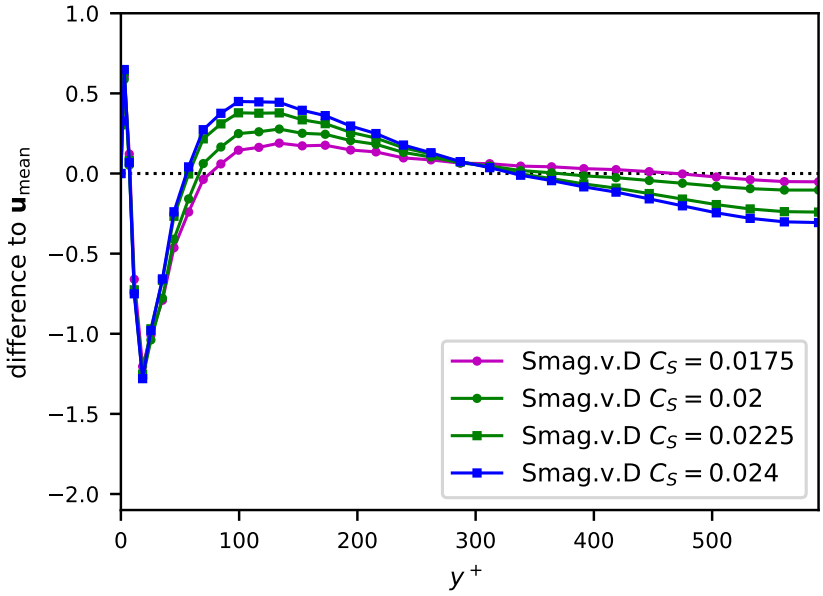

(b) Smagorinsky model van Driest with $C_S = 0.0175$, 0.02, 0.0225 and 0.024

Figure 5.16: $\mathrm{Re}_\tau = 590$, Smagorinsky van Driest model: Comparison between turbulent flow constant in difference to the mean.

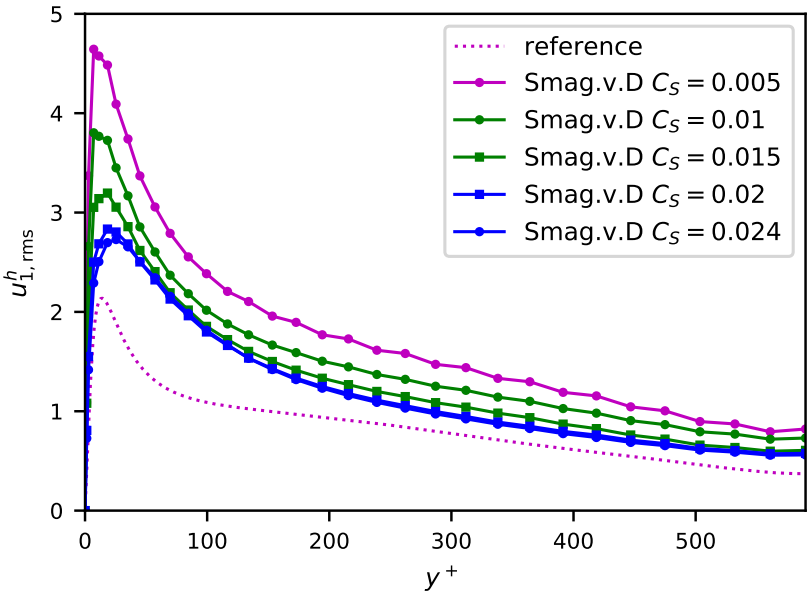

(a) Smagorinsky van Driest model with $C_S = 0.005$, 0.01, 0.015, 0.02 and 0.024

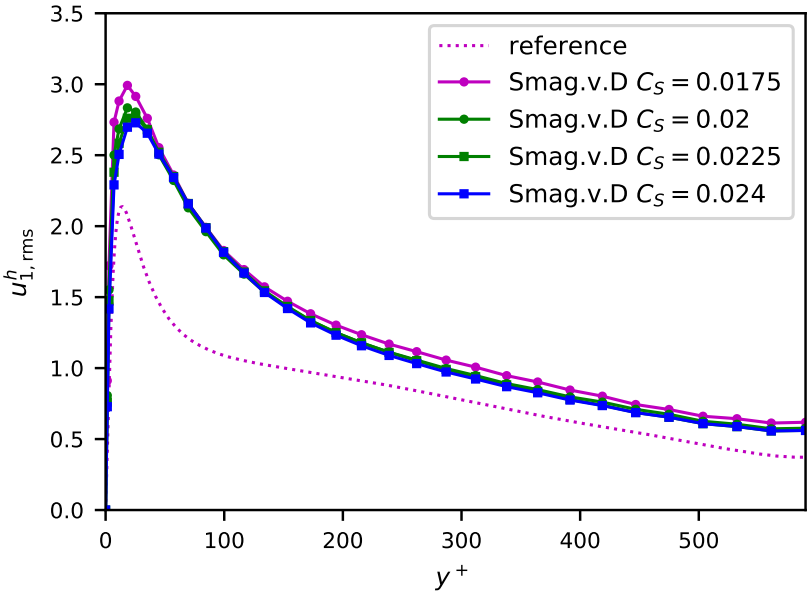

(b) Smagorinsky model van Driest with $C_S = 0.0175$, 0.02, 0.0225 and 0.024

Figure 5.17: $\mathrm{Re}_\tau = 590$, Smagorinsky van Driest model: Comparison between turbulent flow constant in Root Mean Squared tensor.

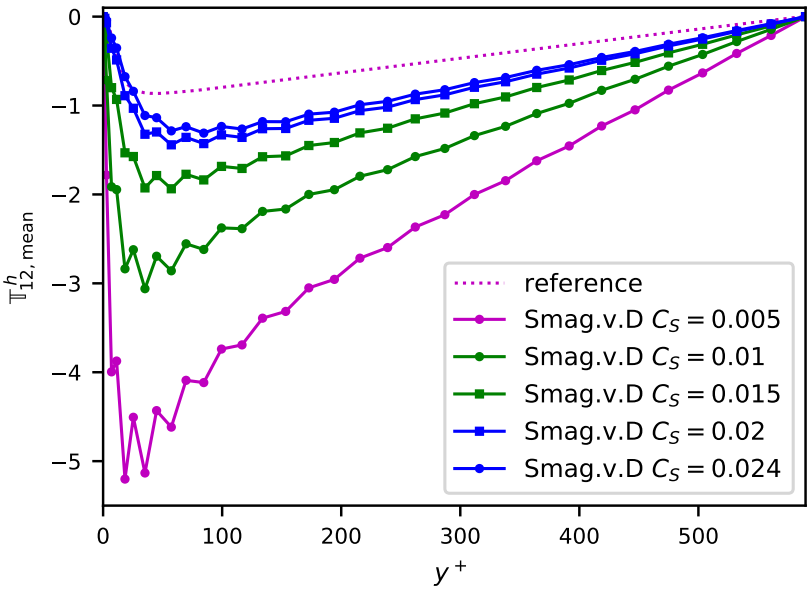

(a) Smagorinsky van Driest model with C_S = 0.005, 0.01, 0.015, 0.02 and 0.024

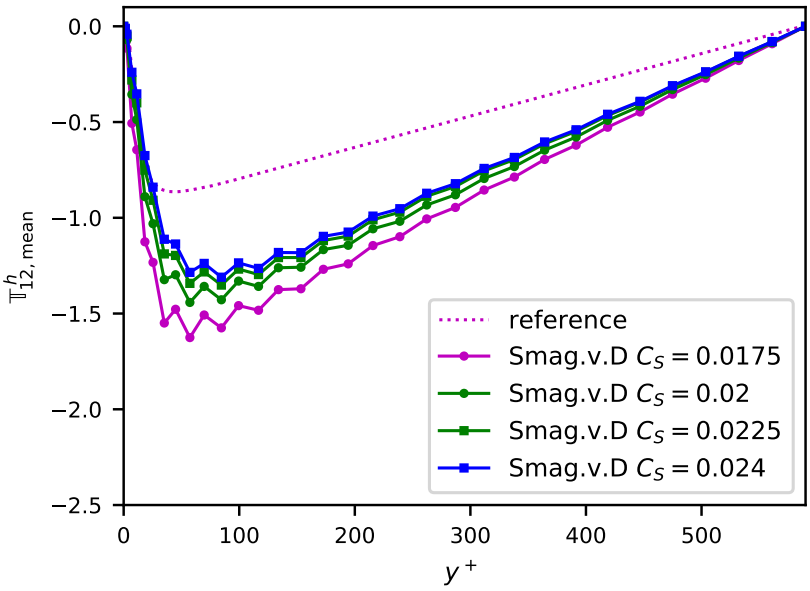

(b) Smagorinsky van Driest model with C_S = 0.0175, 0.02, 0.0225 and 0.024

Figure 5.18: $\mathrm{Re}_\tau = 590$, Smagorinsky van Driest model: Comparison between turbulent flow constant in Reynolds Stress tensor.

The first round turbulent viscosity constants for the Smagorinsky van Driest model are 0.005, 0.01, 0.015, 0.02 and 0.024. We dropped the constants 0.005 and 0.01 for the Smagorinsky model with van Driest Damping after the first round experiments and added 0.0175 and 0.0225. The change of choosing makes progress, since in Figure 5.16(a) and Figure 5.16(b), we can see that the curve 0.0175 goes nearer to the reference line than the curve 0.02. But in Figure 5.17(b) and Figure 5.18(b), the curve 0.0175 belongs no longer to the fittest curves. To this point, we would choose the curve 0.02. Because in the Figure 5.16(b) there is only slightly difference between 0.02 and 0.0175, but in the Figure 5.18(b) we would notice that the curve 0.0175 is much worse than 0.02. Therefore, we choose 0.02 to be the best turbulent viscosity constant in the case $\mathrm{Re}_\tau = 590$ for the Smagorinsky van Driest model.

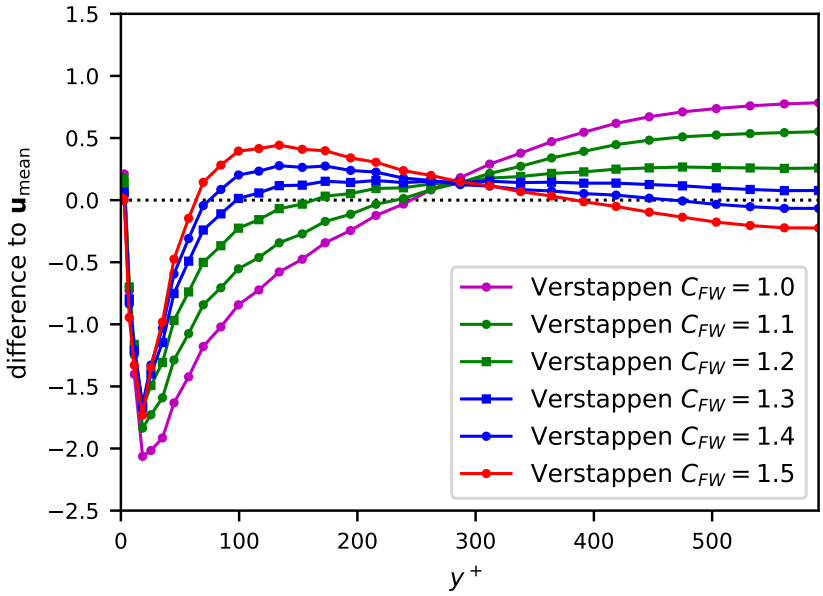

(a) Verstappen model with $C_{FW} = 1.0$, 1.1, 1.2, 1.3, 1.4 and 1.5.

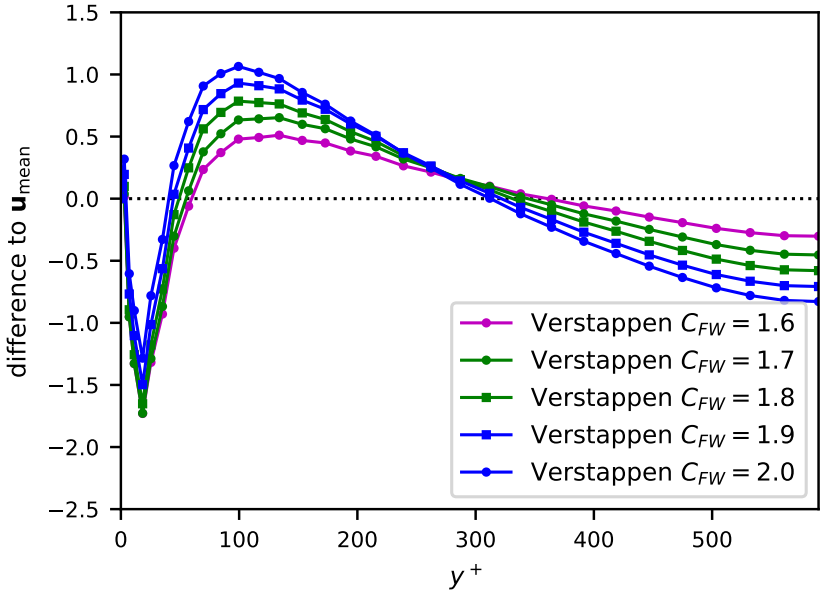

(b) Verstappen model with $C_{FW} = 1.6$, 1.7, 1.8, 1.9, and 2.0.

Figure 5.19: $\mathrm{Re}_\tau = 590$, Comparison in difference to the mean.

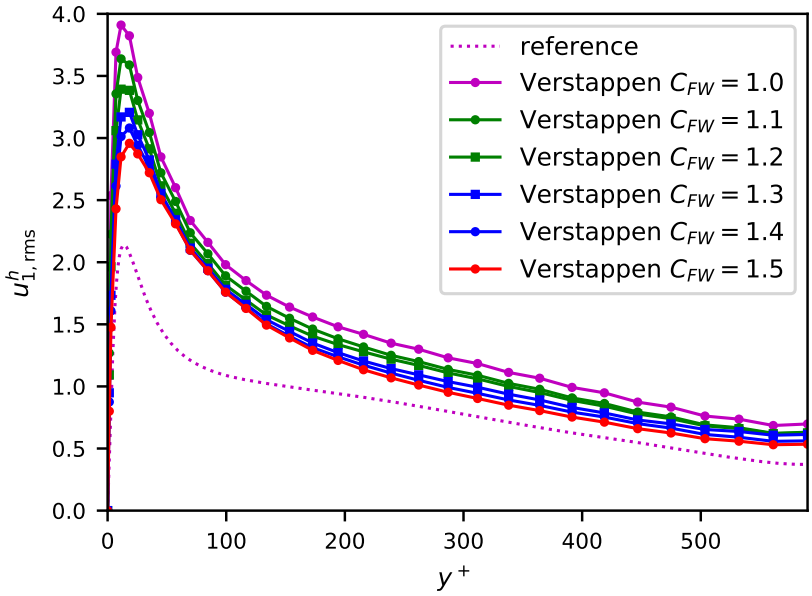

(a) Verstappen model with $C_{FW} = 1.0$, 1.1, 1.2, 1.3, 1.4 and 1.5.

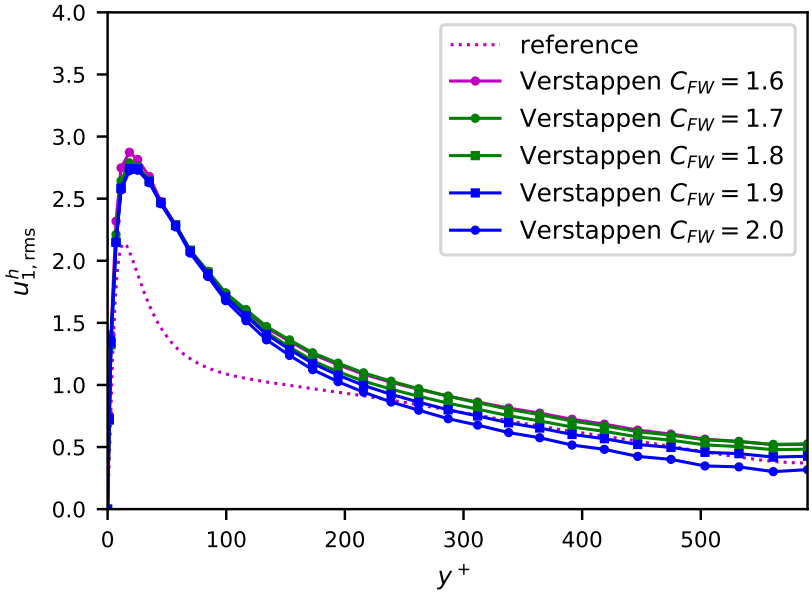

(b) Verstappen model with $C_{FW} = 1.6$, 1.7, 1.8, 1.9, and 2.0.

Figure 5.20: $\mathrm{Re}_\tau = 590$, Comparison in Root Mean Squared tensor.

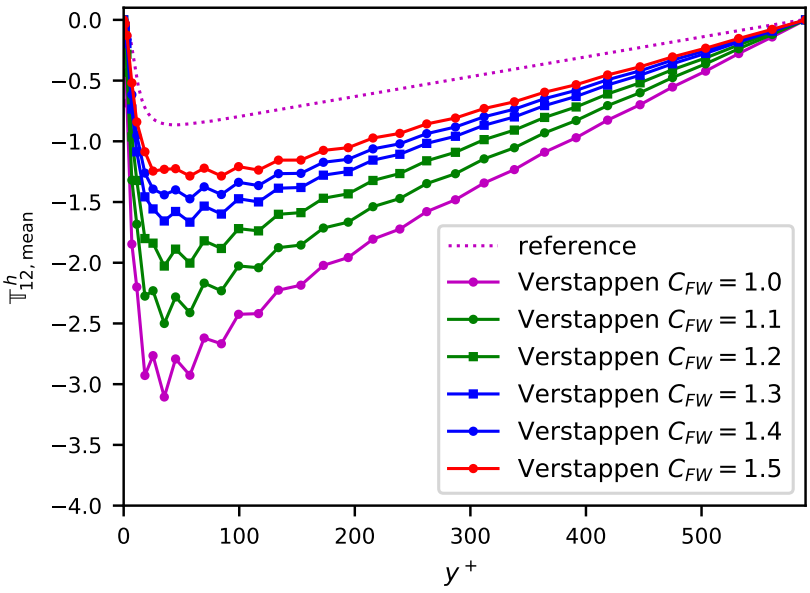

(a) Verstappen model with $C_{FW} = 1.0$, 1.1, 1.2, 1.3, 1.4 and 1.5.

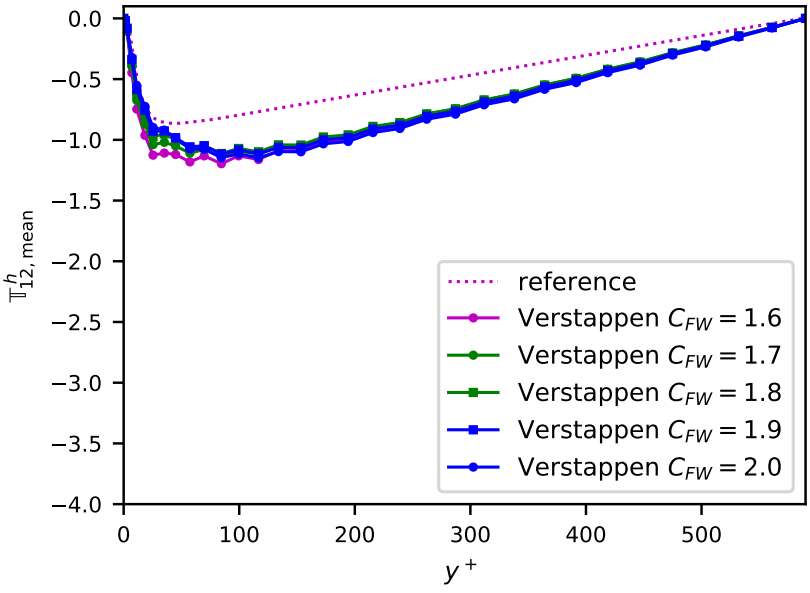

(b) Verstappen model with $C_{FW} = 1.6$, 1.7, 1.8, 1.9, and 2.0.

Figure 5.21: $\text{Re}_\tau = 590$, Comparison in Reynolds stress tensor.

The choice of the filter width constant for the Verstappen model is difficult. We have chosen eleven constants in the interval $[1.0, 2.0]$. And Since it is not clear to show the results, if we put all eleven curves in one figure. We separated them to two groups of the constants. From Figure 5.19(a) and Figure 5.19(b), we can see that the curves 1.3, 1.4 and 1.5 belong to the best choices. And in the Figure 5.20 and Figure 5.21, we find out that 1.5 behaves good. Therefore, we choose 1.5 to be the best filter width in the case $\mathrm{Re}_\tau = 590$ for the Verstappen model.

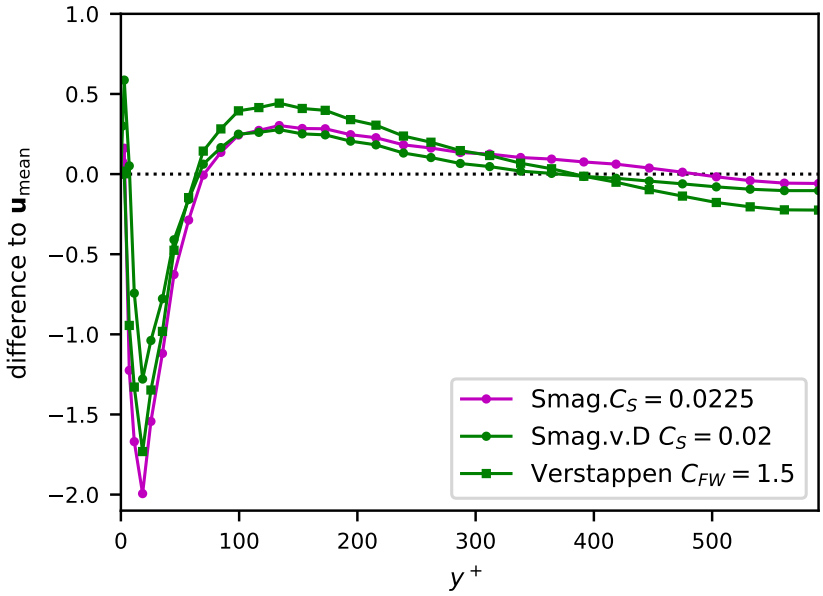

Figure 5.22: $\mathrm{Re}_\tau = 590$, Comparison in difference to the mean.

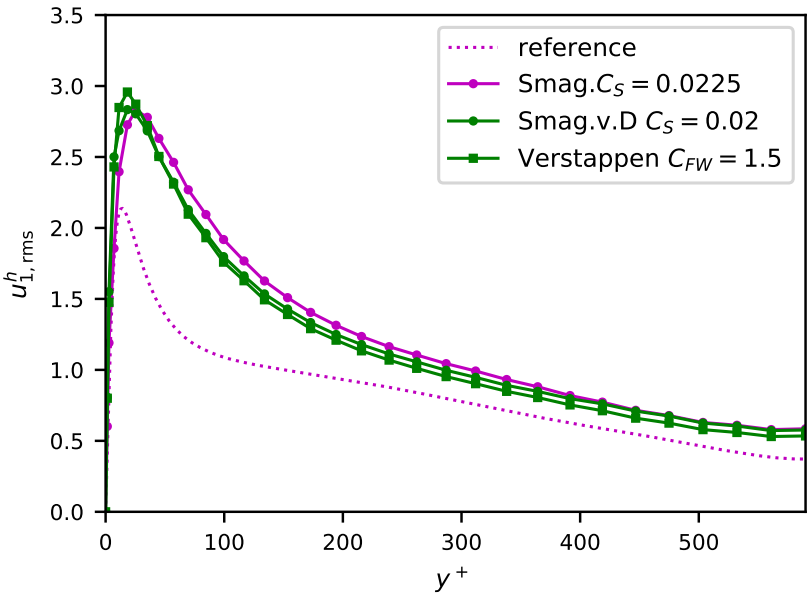

Figure 5.23: $\mathrm{Re}_\tau = 590$, Comparison in Root Mean Squared tensor.

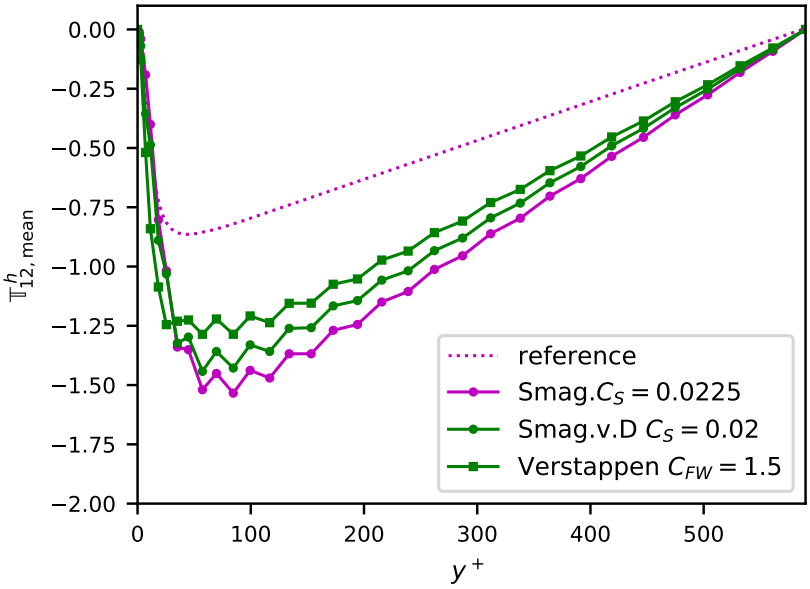

Figure 5.24: $\mathrm{Re}_\tau = 590$, Comparison in Reynolds Stress tensor.

As we have done in the case $\mathrm{Re}_\tau = 395$, we now can compare the curves between the three models. Since we have already chosen Smagorinsky model with $C_S = 0.0225$, Smagorinsky van Driest model with $C_S = 0.02$ and Verstappen model with $C_{FW} = 1.5$. It is clear to put them in the same figure to see which model is better. From Figure 5.22, the Smagorinsky van Driest model is better than other models with respect to the quantity of interest "difference to the mean". We can also conclude from Figure 5.23, that both of the Smagorinsky van Driest model and the Verstappen model are doing well with respect to the quantity "Root mean squared tensor". And for the quantity of interest "Reynolds stress tensor", the Verstappen model is the nearest to the reference curve according to Figure 5.24.

6 Conclusion

This thesis discussed the Navier-Stokes equations and the large eddy simulation for the turbulent flows. We derived the dimensionless Navier-Stokes equations, and gave the initial conditions and the boundary conditions, especially the periodic boundary conditions. We have pointed out that the dimensionless Navier-Stokes equations give us the fundamental simulation of the turbulent incompressible flows. Furthermore, we discussed the classical large eddy simulation. According to the Boussinesq hypothesis, we gave the construction of the Reynolds stress tensor with respect to the turbulent viscosity constant. For the estimation of the turbulent viscosity, we have had a further discussion, since the eddy viscosity model is nonlinear. In this thesis, we gave two methods to model the turbulent viscosity, which are the Smagorinsky model and the Verstappen model.

The Smagorinsky model is a symmetric model, which adds the turbulent viscosity model ν_T to the momentum equation of the Navier–Stokes equations. And the turbulent viscosity model of the Smagorinsky model ν_T depends on the dimensionless Smagorinsky coefficient C_S and the local mesh width δ. On the other side, the Verstappen model considers a sub-filter which filters out the eddies of size smaller than the average scale. The sub-filter is an essential step which helps us to construct the eddy viscosity model of the Verstappen model. And the eddy viscosity model of the Verstappen model depends on $r = -\frac{1}{3}\mathrm{tr}(\mathbb{D}^3)$ and $q = \frac{1}{2}\mathrm{tr}(\mathbb{D}^2)$, where $\mathbb{D} = \mathbb{D}(\boldsymbol{v})$ represents the deformation tensor of the velocity. And the eddy viscosity model of the Verstappen model depends on the mesh width δ as well. The approximation of r and q is based on Poincare's inequality. By applying Lemma 1 and Lemma 2, we can give a proper upper-bound of the eddy viscosity model of the Verstappen model.

For the numerical studies, we introduced the variational multiscale method, precisely the three-scale coarse space projection-based VMS method. We discussed the finite element spaces that we need for the simulation. The finite element method space for the velocity is continuous quadratic polynomials and for the pressure is discontinuous linear polynomials on hexahedra. We also defined in this case the periodic boundary conditions.

In the book [2], two examples of the turbulent flow problems were mentioned, which were $\mathrm{Re}_\tau = 180$ and $\mathrm{Re}_\tau = 590$. In the same time, the Verstappen model was stated to be successfully tested for the turbulent channel flow under $\mathrm{Re}_\tau = 590$ in paper [7]. Therefore, in this thesis, we performed two cases $\mathrm{Re}_\tau = 395$ and $\mathrm{Re}_\tau = 590$, governed by the dimensionless incompressible Navier–Stokes equations. We applied the Smagorinsky model, the Smagorinsky van Driest model and the Verstappen model with the code ParMooN. And we have chosen three quantities of interest to compare the simulations, which were the difference to the mean, the Reynolds stress tensor and the root mean

squared tensor.

From the results of the experiments, we can see that, according to the three quantities of interest, we cannot say there is a model that is absolutely better than the others. However, the Smagorinsky van Driest model and the verstappen model both have a better behavior. In the sense of difference to the mean, the Verstappen model with the filter width 1.5 is better the other models when $\mathrm{Re}_\tau = 395$. When $\mathrm{Re}_\tau = 590$, the Smagorinsky model with van Driest damping is clearly better the other two models. And in the sense of the Reynolds stress tensor, the Smagorinsky model is always better than the other two models. Another point to be noticed that, the Smagorinsky model and the Smagorinsky van Driest model have different best choice of the constants as the setting of Re_τ changes.

Bibliography

[1] Dongho Chae. "On the spectral dynamics of the deformation tensor and new a priori estimates for the 3D Euler equations". In: *Comm. Math. Phys.* 263.3 (2006), pp. 789–801.

[2] Volker John. *Finite element methods for incompressible flow problems.* Vol. 51. Springer Series in Computational Mathematics. Springer, Cham, 2016, pp. xiii+812.

[3] Volker John. "On large eddy simulation and variational multiscale methods in the numerical simulation of turbulent incompressible flows". In: *Appl. Math.* 51.4 (2006), pp. 321–353.

[4] Volker John and Michael Roland. "Simulations of the turbulent channel flow at $\mathrm{Re}_\tau = 180$ with projection-based finite element variational multiscale methods". In: *Internat. J. Numer. Methods Fluids* 55.5 (2007), pp. 407–429.

[5] A. Kolmogoroff. "The local structure of turbulence in incompressible viscous fluid for very large Reynold's numbers". In: *C. R. (Doklady) Acad. Sci. URSS (N.S.)* 30 (1941), pp. 301–305.

[6] B. Mohammadi and O. Pironneau. *Analysis of the k-epsilon turbulence model.* RAM: Research in Applied Mathematics. Masson, Paris; John Wiley & Sons, Ltd., Chichester, 1994, pp. xiv+196.

[7] Volker John Naveed Ahmed. "An Assessment of Two Classes of Variational Multiscale Methods for the Simulation of Incompressible Turbulent Flows". unpublished.

[8] P. Ploumhans et al. "Vortex methods for direct numerical simulation of three-dimensional bluff body flows: application to the sphere at Re = 300, 500, and 1000". In: *J. Comput. Phys.* 178.2 (2002), pp. 427–463.

[9] Roel Verstappen. "When does eddy viscosity damp subfilter scales sufficiently?" In: *J. Sci. Comput.* 49.1 (2011), pp. 94–110.

Freie Universität Berlin

Selbstständigkeitserklärung

Name	Liu
Vorname	Mingyang
geb. am	17.10.1990
Matr. Nr.	4965440

Ich erkläre gegenüber der Freien Universität Berlin, dass ich die vorliegende masterarbeit selbstständig und ohne Benutzung anderer als der angegebenen Quellen und Hilfsmittel angefertigt habe.

Die vorliegende Arbeit ist frei von Plagiaten. Alle Ausführungen, die wörtlich oder inhaltlich aus anderen Schriften entnommen sind, habe ich als solche kenntlich gemacht.

Diese Arbeit wurde in gleicher oder ähnlicher Form noch bei keiner anderen Universität als Prüfungsleistung eingereicht und ist auch noch nicht veröffentlicht.

Datum: December 19, 2019 Unterschrift:

Mingyang Liu